行政院國家科學委員會專題研究計畫 成果報告

智慧型生物訊號誘導藥物釋放系統前瞻研究:以癲癇症為模式--應用於訊號誘導藥物釋放系統之智慧型生醫複合材料結構製程與性質研究(總計畫及子計畫二)(3/3)
研究成果報告(完整版)

計 畫 類 別 ： 整合型
計 畫 編 號 ： NSC 98-2627-B-009-001-
執 行 期 間 ： 98 年 08 月 01 日至 99 年 10 月 31 日
執 行 單 位 ： 國立交通大學材料科學與工程學系（所）

計 畫 主 持 人 ： 陳三元
共 同 主 持 人 ： 黃國華

報 告 附 件 ： 出席國際會議研究心得報告及發表論文

處 理 方 式 ： 本計畫可公開查詢

中 華 民 國 99 年 10 月 27 日

行政院國家科學委員會補助專題研究計畫成果報告

智慧型生物訊號誘導藥物釋放系統前瞻研究:
以癲癇症為模式-（3/3）

計畫類別：□ 個別型計畫　　■ 整合型計畫
計畫編號：
執行期間：　98　年　8月　1　日至　99　年　7　月　30　日

總計畫主持人：陳三元　國立交通大學材料科學與工程學系
子計畫主持人：
梁勝富　國立成功大學資訊工程系
陳三元　國立交通大學材料科學與工程學系
蕭富仁　國立成功大學認知科學所

成果報告類型(依經費核定清單規定繳交)：□精簡報告　■完整報告

本成果報告包括以下應繳交之附件：
□赴國外出差或研習心得報告一份
□赴大陸地區出差或研習心得報告一份
□出席國際學術會議心得報告及發表之論文各一份
□ 國際合作研究計畫國外研究報告書一份

處理方式：除產學合作研究計畫、提升產業技術及人才培育研究計畫、列管計畫及下列情形者外，得立即公開查詢
■涉及專利或其他智慧財產權，□一年■二年後可公開查詢

執行單位：國立交通大學材料科學與工程學系

中　華　民　國　99　年　10　月　24　日

智慧型生物訊號誘導藥物釋放系統前瞻研究:以癲癇症為模式-總計畫成果報告(3/3)

Frontier Research on Smart Biologically-Stimuli Drug Delivery System Based on Epilepsy –

執行期限：98 年 8 月 1 日至 99 年 7 月 31 日
總計畫主持人：陳三元　國立交通大學材料科學與工程學系
子計畫主持人：梁勝富　國立成功大學資訊工程系
陳三元　國立交通大學材料科學與工程學系
蕭富仁　國立成功大學認知科學所

Abstract

In the third year, the aim of this subproject is to develop a smart system which is responsible to sense or detect the need of patients by monitoring and analyzing patient's (through the use of an animal model) abnormal discharge due to epilepsy and to translate a control signal to the drug delivery device. For **Sub-Project-1**, (1) an on-line seizure detection method applicable to multiple seizure types has been developed. To evaluate the usefulness of the proposed method, it was applied to the continuous EEG of four Long-Evans rats with spontaneous absence seizures and of four Wistar rats with epileptiform activities induced by pentylenetetrazol (PTZ). For subject dependent evaluation, the average seizure detection rate, false detection rate, and detection delay time were 98.2%, 8.9%, and 0.51 s for absence seizures, respectively, and were 97.3%, 6.6% and 0.53 s for PTZ induced seizures, respectively. (2) A wireless behavioral state and physiological signal monitoring system. It demonstrates successful observation of kindle process of temporal lobe epilepsy and discrimination vigilance states. To integrate with subproject-1 and subproject-3, two major studies were focused in the third year for **Sub-Project-2**. Firstly, electrically-responsive drug elution behavior of the hybrid hydrogel based on an amphiphilic chitosan and inorganic silicawas characterized and evaluated systematically in-vitro using an anticonvulsant drug, ethosuximide, as model molecule. Secondly, further integrating the hybrid hydrogel, designed as a chip-like drug reservoir, with an automatic self-detection and signal transmitter system, applying to a rat's model, the resulting seizure frequency was considerably reduced and has experimentally proved that such a self-detection chip-like drug delivery device holds promising prospective in practical epileptic treatment. **Subproject-3** reported that when ESM injected into lateral cortical region (A0L5), the number and total duration of SWDs were remarkably decreased and the onset of

SWDs was prolonged. The data will be benefit for the nanoparticle construction of the **SubProject-2** and closed-loop design of the **SubProject-1** being crucial for the test of a close-loop seizure controller. In addition, comparison of effects of intracortical infusion of saline or ESM into 3 brain sites (A0L5, and A0L2) in SWDs of Wistar rats induced by pentylenetetrazol (PTZ) (20 mg/kg, i.p.). **Therefore, the seizure detector developed in this subproject 1 was also integrated with the drug delivery device developed in subproject 2 to perform a responsive drug delivery system and this system was evaluated by the rat models developed in subproject 3. The drug delivery system consists of four units: (a) signal acquisition and amplification unit, (b) 8051 micro-processor and wireless data transmission unit, (c) electric field and drug delivery chip, (d) host system for data storage and real-time display. It was demonstrated on the in vivo test and the experimental results show that the spike and wave discharges of the rats reduced by nearly 50% while ethosuximide (ESM) was released from the self-detection drug delivery system.**

Keywords: On-line seizure detection, Drug delivery system, Epilepsy, Electrically-responsive

I. Introduction

Up to now, there is no true control of release of drug after administrated into human body, because the drug is released solely by a pre-design of the host matrix and its corresponding environment. Therefore, it is more technically desirable and therapeutically effective to develop the drug delivery system on the bio-compatible substrate to detect the need of patient according to the disease state of patients in particular for chronic diseases such as epilepsy.

Based on the idea, this research project uses epilepsy, i.e., a model disease, as an in-vivo platform for proper evaluation of drug delivery device. The drug delivery system with a non-implantable prototype is expected to be investigated, including a controllable burst drug delivery device designed specifically for epileptic syndrome, signaling and correlating the biological wave with a mechanical micro-deformation of a novel smartgel membrane, establishing a controlled burst release with precision dose analogue with natural secretion burst behavior in human body, and establishing smart interface to convert and model the behavior between pathological analog input into digitally readable data, etc. will be systematically evaluated and characterized in the 3 sub-projects.

II. Progress report (計畫執行進度)

(1) Sub-Project-2:

Development and characterization of smart responsive biomedical composite structure for drug delivery system

P-1 Preparation of CHC Hydrogels

To prepare CHC hydrogels, the preparation procedure is separated into two stages, the first stage is to prepare three suspensions; (1) 1.3% w/v CHC solution by suspending the above-mentioned CHC samples in deionized water at 25 ^{o}C for 24 hours. (2) 1% w/v GP (genipin, Challenge Bioproducts Co., Ltd., Taiwan) solution which is prepared by dissolving GP powders in deionized water stirring for 2 hours at 50^{o}C to ensure that GP was fully dissolved, and (3) acid-hydrolyzed TEOS solution by mixing TEOS, together with ethanol and H_2O with different weight ratios ([TEOS]:[H2O]:[Ethanol]=1:5:7, 2:5:7, and 1:10:14 separately), and HCl, in order to give a final silica-containing CHC hybrid structure. After that, the GP and TEOS solutions with different weight ratios were added to the CHC solution while stirring for 30 minutes, followed by incubating at 50^{o}C for 2 days. Thus, the genipin-cross-linked CHC-TEOS hybrid hydrogels were formed and designated as GP*x*TEOS*y,* where the symbol *x* and *y* represent the weight ratios (in percentage) in the dried hydrogel. The synthetic parameters of hybrid hydrogels are listed in Table 1.

Table 1. The synthesis parameters of CHC-TEOS hydrogels designated as GP*x*TEOS*y,* where the symbol *x* and *y* represent the weight ratio in the dried hydrogel.

CHC Hydrogel	1.3 % w/v $CHC_{(sol)}$(g)	1% w/v $GP_{(sol)}$(g)	TEOS (g)
GP0TEOS54	2	0	0.03
GP0.5TEOS54	2	0.03	0.03
GP1TEOS54	2	0.06	0.03
GP1.5TEOS54	2	0.12	0.03
GP1.5TEOS0	2	0.12	0
GP1.5TEOS27	2	0.12	0.018
GP1.5TEOS54	2	0.12	0.03
GP1.5TEOS70	2	0.12	0.045

The swelling behaviors of the hybrid hydrogels with different degrees of cross-linking by genipin and TEOS are illustrated in Figs. 1(a) and (b), respectively. The profiles of GP0TEOS54 and GP1.5TEOS0 showed some specificity that both swollen hybrid hydrogels were hard to reach the swelling equilibrium but tended to collapse while immersing into water over a short period of time. It has known from previous study that CHC exhibits an excellent water affinity behavior at pH 7.4. In the absence of any crosslinking agents, the CHC was found

to swell extensively till reaching a structural failure (collapse). Such structural failure is probably resulting from dis-assembly of the CHC polymer chains as a result of dissolution to form micelle entities in water. Similar structural dis-assembly was also observed from the hybrid hydrogels using either 54% TEOS alone or 1.5% genipin, as given in Figs. 1(a) and 6(b), respectively. It is then suggested that the hybrid hydrogels containing either TEOS or genipin alone were still subjecting to collapse upon extensive water absorption. However, what is more interesting is that the swelling behavior for the hybrid hydrogels with the use of both TEOS and genipin such as samples of GP0.5TEOS54, GP1TEOS54, GP1.5TEOS54, GP1.5TEOS27, GP1.5TEOS54, and GP1.5TEOS70, as given in Figs. 1(a) and (b), reaches equilibrium state for a longer time period of 45 minutes before a final structural collapse occurred. That is to say, the presence of both TEOS and genipin in the hybrids has more pronounced effect to strengthen the structure of the hybrids from undesirable mechanical failure upon swelling than their individual contribution. As such, the swelling equilibrium can be achieved over a prolonged duration while structure integrity remained identical, rather than collapsed upon extensive swelling.

However, increase in the concentration of both genipin and TEOS decreased the swelling ratio of the resulting hybrid hydrogels. The swelling behavior in Fig. 1(a) indicates that samples of GP0.5TEOS54, GP1TEOS54, and GP1.5TEOS54 (i.e., hybrids with constant TEOS) have a swelling ratio, decreased with genipin content, of 427%, 354%, and 269% respectively. For samples with constant genipin, GP1.5TEOS27, GP1.5TEOS54, and GP1.5TEOS70 having a swelling ratio, decreased with TEOS content, of 550%, 326%, and 300%, respectively. It is then concluded that the higher content of the crosslinkers, the lower the swelling capability of the CHC hybrids results. The mesh size of the swollen CHC chains should accordingly be reduced proportionally.

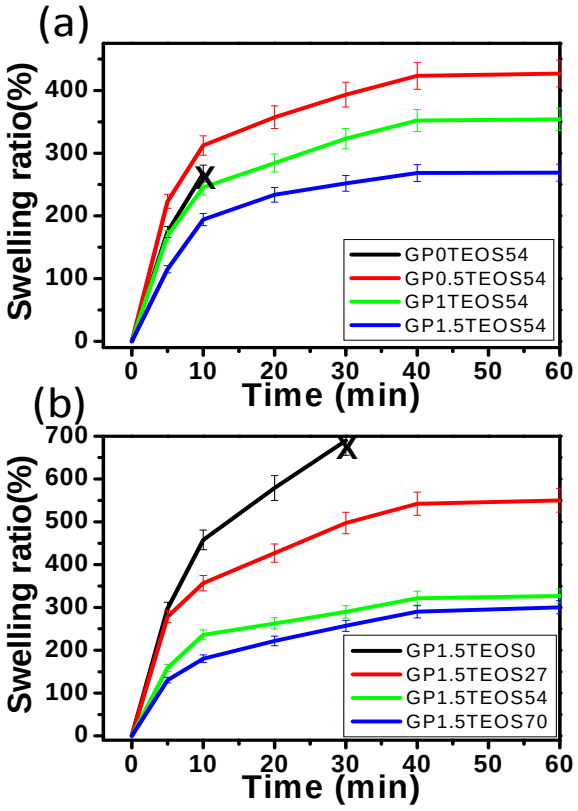

Fig. 1. Swelling behavior of the hybrid hydrogels with different contents of (a) genipin and (b) TEOS, as a function of time.

P-2: Assembly of the Drug Delivery Device and Drug Release

The drug delivery device is designed by combination of hybrid hydrogels and a transparent, plastic container. Fig. 2(a) is a schematic flowchart which demonstrates the procedures to prepare the device. A transparent plastic container, made of poly (methyl methacrylic acid) (PMMA, YEONG-SHIN Co., LTD, Taiwan) has dimensions of 2cm x 2cm x 0.2cm with a single small opening of 0.2 mm in diameter on one side of the container, whilst the other three sides were mechanically sealed the PMMA plates. The one with the small opening is designed as the outlet for drug elution. Two rectangle-shaped platinum plate (Pt, YEONG-SHIN Co., LTD, Taiwan, 4cm x2cm x 0.1mm in dimension) were placed in a constant distance with two parallel sides of the acrylic container as electrodes. After the hybrid hydrogels was inserted into the container described above and sealed, a chip-like device was successfully produced (Figs. 2(a) and (b))

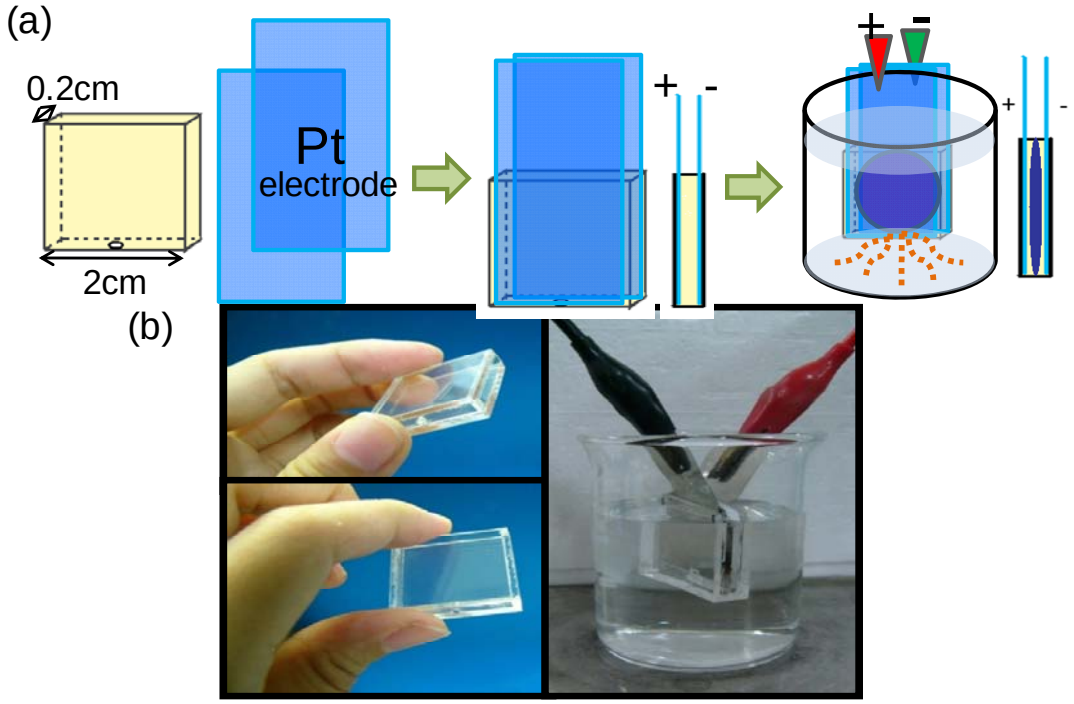

Fig. 2. (a) Schematic flowchart for chip-based hybrid device preparation (b) The setup of hybrid device where an electrical field of different strengths can be generated between the Pt electrodes in the sealed container.

Drug release test was carried out by first incorporating the hydrophilic anticonvulsant drug, ethosuximide (ESM), of concentration 15mg/ml, into the CHC solutions. The drug was

dissolved completely in the presence of CHC-containing solution with a concentration of 1.5 wt%. Then after vigorously stirring, the final ESM-containing solution was cast in a petri dish and dried in oven at 50°C to form resulting membrane-like hydrogels according to the preparative procedures aforementioned.

The ESM-loaded hybrid hydrogel with dimensions of 30 mm in diameter and 0.3 mm in thickness, on a dried basis, was kept in space between two platinum electrodes. Then, together with the final device, immersed into a glass beaker contained 50-ml distilled water. The device was then exposed under an electric voltage generated by a dc power source over a range of 0V, 15V, 30V, and 60V. At appropriate time intervals, 2 ml solution was extracted from the beaker and analyzed using a UV spectrophotometer (Evolution 300) at a specific wavelength λ=254 nm.

ESM is water soluble and thermally stable drug, which is suitably employed for controlled release study and was employed as model molecule in this work. The in-vitro release of ESM from the CHC hybrids was measured over a 60-min period in deionized water, as shown in Figs. 3(a) and (b). CHC hybrids with either TEOS or genipin alone illustrated a burst-like profile where the ESM was nearly completely eluted within 15 minutes. However, for hybrids such as GP0.5TEOS54, GP1TEOS54, GP1.5TEOS54, GP1.5TEOS27, GP1.5TEOS54, and GP1.5TEOS70 exhibited much slower release profile when both TEOS and genipin were incorporated with a higher concentration in either genipin or TEOS into the hybrids. The slower release profile for the hybrids with higher crosslink density can be resulting from a smaller mesh size of the hybrid networks than those hybrids with lower or little crosslink. The evolution of smaller mesh size in the network structure of high-crosslink hybrids may then be used to explain a lower diffusion rate for the ESM molecules to eluting outward. Hence, manipulation of the nanostructure of the hybrids has become a very important issue for designing a device suitable for controlled release of ESM.

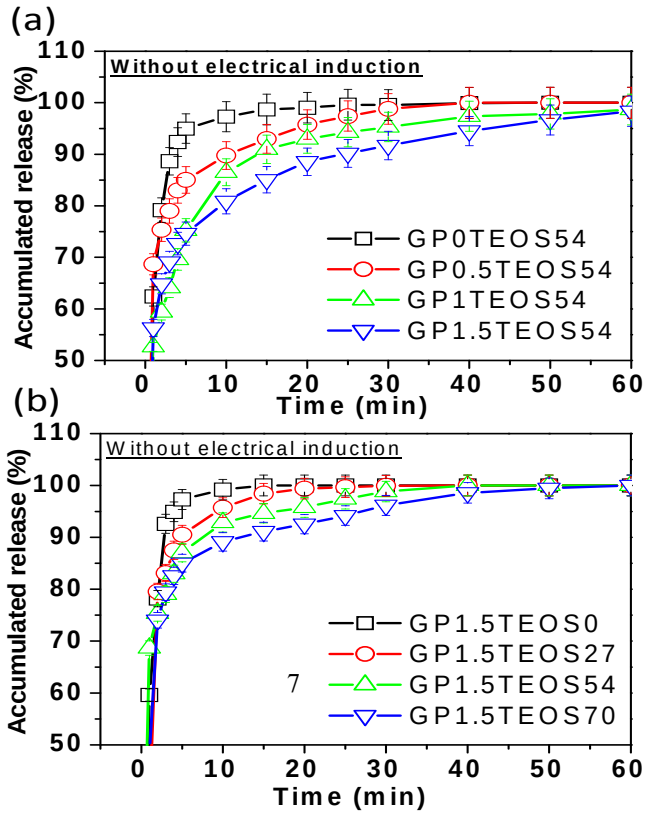

Fig. 3. In-vitro release of ESM from the hybrid hydrogels with **(a)** different genipin contents and **(b)** different TEOS contents.

P-3: Drug Release Behavior of the Device under Electric Field

I. Effect of genipin

Figure 4(a) shows the in-vitro release of ESM from GP0TEOS54 hybrid which was integrated into a membrane-like configuration (hereinafter termed "chip"), under an applied electric field of different DC voltages from 0V to 60 V. It can be observed that the ESM was completely depleted over a time period of 120 minutes under zero voltage. Compared to Fig. 3(a), it indicates that when the hybrid hydrogels were inserted into the closed container, a full-scale swelling of the hybrids was effectively inhibited due to a constrained space. Since the swelling of the hybrids sandwiched in the container is heavily restricted, a subsequently restriction of the drug diffusion out of the chip is expected as a result of smaller mesh size developed within the hybrid hydrogel, resulting in a much slower release kinetics.

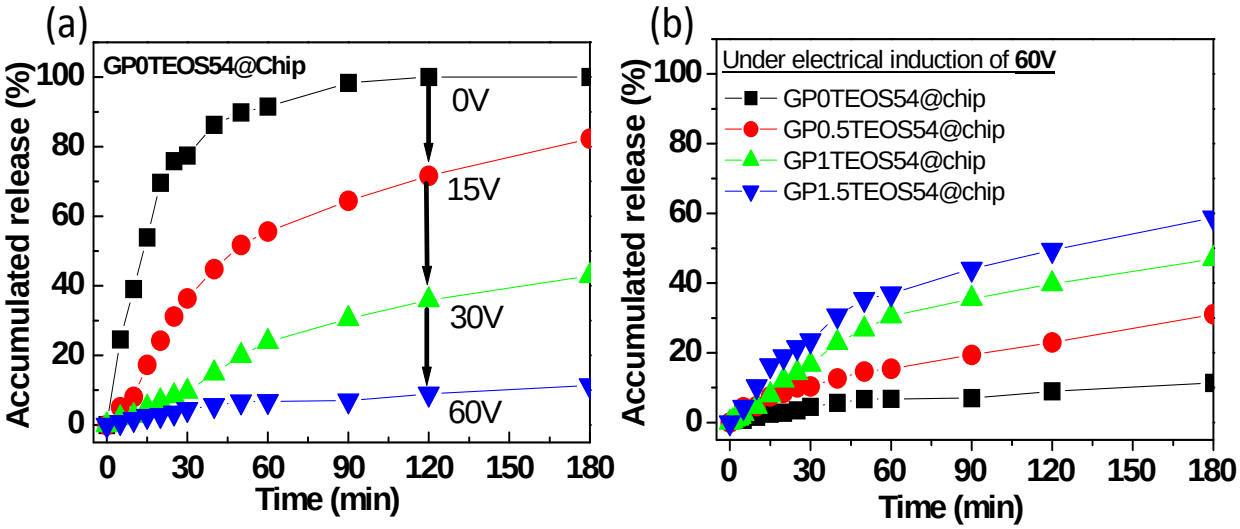

Fig. 4. (a) The ESM release profiles from GP0TEOS54 when applied DC electric field was operated as 0V, 15V, 30V, and 60V. (b) The release profiles with different genipin content under electrical operation of 60V.

Under electrical stimulus at voltages of 15V, 30V, and 60V respectively, drug release was restricted considerably with increased voltage, where only ~15% of ESM being eluted over a period of 180 minutes under 60-V electrical stimulus. Such an electrical-field-modulated ESM

release profile can be presumably considered as a result of both electrophoretic and electroosmotic actions interplaying between the hybrid and ESM.

The chemical structure of ESM, with a molecular mass of 141.2 g/mole, has a chiral framework containing a five-member ring, with two negatively charged carbonyl oxygen atoms with a ring nitrogen between them and one asymmetric carbon atom, as shown in Figure 5. Normally, it is more stable for ESM to perform with the structure of dehydrogenation. It means that the electron resonance between two carbonyl oxygen atoms and dehydrogenated nitrogen atom will give rise to a negatively charged ESM, which has been verified by ELS where its zeta potential is given in Table 2. Hence, upon application of an electrical stimulus, the H^+ ion, located at the nitrogen of ESM, preferred to escaping and being reduced at the cathode surface. In the meantime, the ESM molecules, which lost proton, should display electrophoretic movement to the anode because of strong negative charges. On the other hand, the immobile negative charges on the CHC polymer chain are exposed to an attractive force to positively charged H^+ ions formed as a result of the electrolysis of water or dehydrogenation of ESM in the presence of electric voltage. These H^+ ions forming a cloud of ions will enclose the polymers. Upon the application of electrical voltage, the positive H^+ ions surrounding the polymers will begin to move toward the anode with attractive force. Then the water molecules together with the ESM will be dragged toward the cathode by ion flow according to the gradient of ion and osmotic pressure, forming electroosmosis flow. Since the two forces, electrophoresis and electroosmosis, drive ESM movement toward the opposite direction, the net release of the drug from the hybrids is largely restricted (Fig. 5)**.** Hence, electric current decreased the rate of drug release. With the increase of the applied voltage, those aforementioned effects turned out to be more pronounced, giving rise to a much slower rate of drug release. Therefore, it can be concluded that the electric field provided a net constrained force for ESM to diffuse out of the chip due to the interactive actions of both electrophoresis and electroosmosis.

Moreover, with an increase in genipin, the release profiles under electrical stimulation at 60V, in Fig. 4(b), show a faster release pattern. This observation is contrary to that in the absence of electrical stimulus. This behavior can be explained that at acidic condition, genipin reacted with primary amino groups on chitosan to form heterocyclic amines, the reaction will reduce the positive charges on the polymer chains. It is reasonably to believe that the same reaction scenario can be re-produced in the CHC chain. On this basis, higher crosslink density of the CHC chains with genipin leads to a stronger negatively charged CHC polymeric network. Thus, the effect of electroosmosis, which also facilitates gel shrinkage, should be enhanced, as has been verified. Under such an action, the ESM is forced to move outward the hybrids, and the chip as well, leading to a faster release profile as the genipin content increased.

Table 2. Zeta potential of Ethosuximide at different pH values.

pH values	Zeta potential of ESM (mV)
4	-9.82
7	-21.2

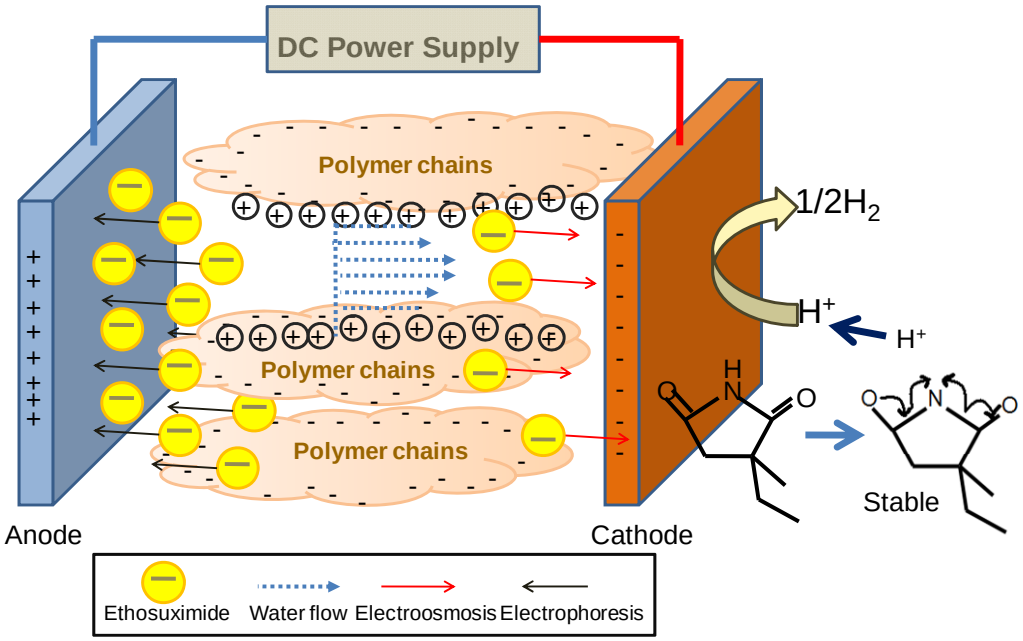

Fig. 5. The schematic drawing shows the influence of applied electrical voltage upon interactive actions between the ESM and CHC chain.

II. Effect of TEOS

Fig. 6(a) shows the elution of ESM from the GP1.5TEOS0-containing chip when the electric field with different voltages was applied. The release profile shows a complete depletion of the drug over a time period of 120 minutes**,** which is much slower than those illustrated in Fig. 3(b), where increase in the TEOS in the hybrids causes a decrease in the release profile. Such a change in ESM elution behavior as a function of TEOS content is also similarly observed in the case aforementioned, where, for the former, the swelling of the hybrids is largely restricted in the presence of TEOS and thus, reduced considerably the ESM diffusion from the hybrids.

Under electrical stimulus at 15V, 30V, and 60V, drug release rate was getting slower with the increase of voltage. This behavior can also be explained as an interplay between electrophoretic and electroosmosis actions aforementioned. The electrophoretic flow of ESM

moves toward the anode but the electroosmotic flow carrying ESM toward the cathode, the opposite and competing actions restrict drug flow considerably out of the chip, resulting in a decreased ESM elution profile.

However, there seems to have an upper limit for the TEOS content in terms of the ESM elution behavior because from experimental observation, shown in Fig. 6(b), a continuous increase of TEOS to a certain critical level, i.e., 54 wt%, in the hybrid, the ESM elution turned faster, which is exactly contrary to what was detected for the hybrids without electrical stimulus. Such a finding can be explained that a more negative charge imparted to the CHC polymeric networks when more TEOS or silica was incorporated. The action of electroosmosis is then enhanced, which further contracts the resulting hybrid hydrogel to a certain extent under identical electric voltage, thus, resulting in a faster ESM elution rate.

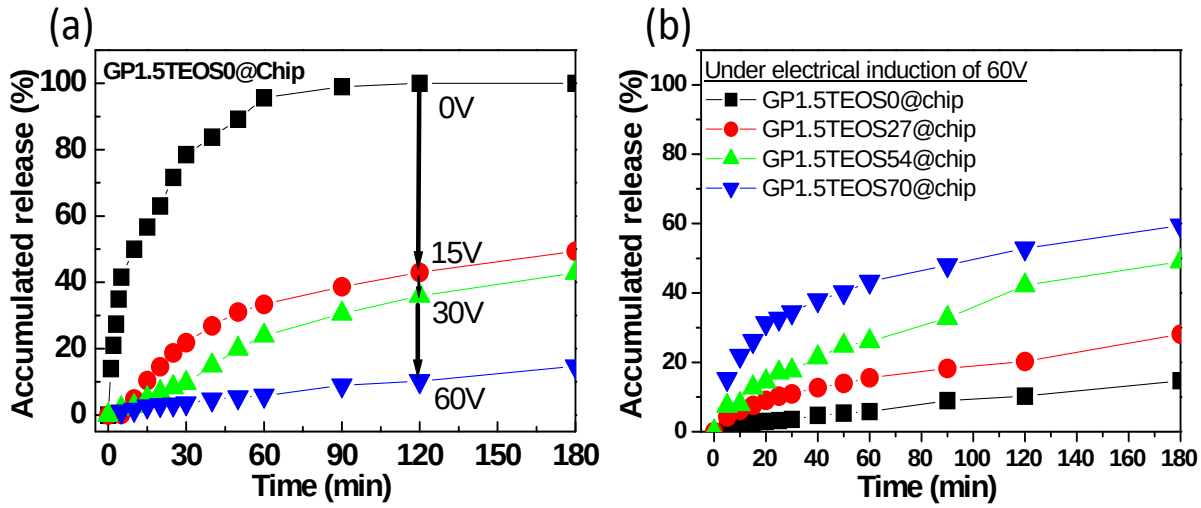

Fig. 6. (a) The ESM release profiles from GP0TEOS54 when applied DC electric field operated at 0V, 15V, 30V, and 60V. (b) The release profiles with different genipin content under electrical operation of 60V.

(2) Sub-project-1:

Detection of pathological signals, and output command processing for drug-delivery system

P-1: ***Experiment 1. Effects of original ESM and ESM with nanoparticles in SWDs***

Figure 7 depicts representative examples of SWDs in the administration of saline, ESM, ESM_SAIO, and ESM_TSAIO. SWDs showed no obvious difference. In this part experiment, we recorded 1-hour spontaneous brain activity before the treatment (baseline) and another 1-hour spontaneous brain activity 30 minutes after the treatment. The indexes were normalized by average of the two 1-hour baselines. Thus, the normalized number of SWDs and total duration of SWDs in 1-hour recording were calculated as indexes to assess the drug effect. In the conditions of administering ESM_SAIO and ESM_TSAIO, rats were restrained in a plastic box then put into the center of a coil that connects with an induction heat machine (EN-35, Taiwan) to destroy the nanoparticle capsule then release ESM. In their control groups, rats were restrained in plastic box then put into the center of a coil without turning on the heat machine.

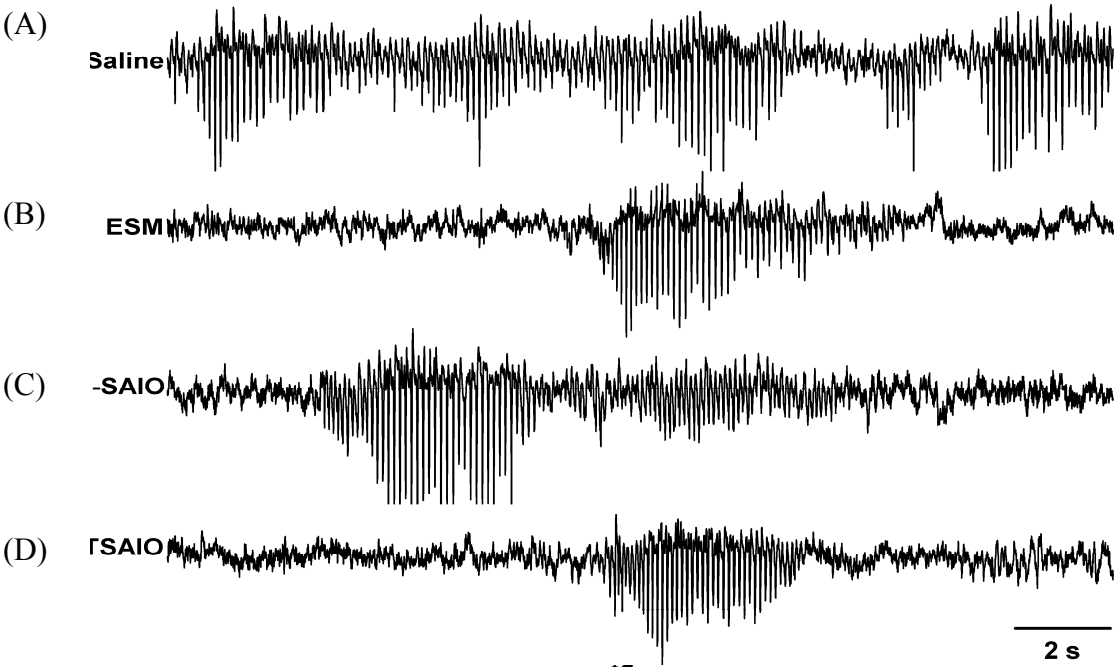

Fig. 7. Representative examples of spontaneous SWDs under intrapeneal administration of saline (A), ethosuximide (ESM) (28 mg/kg, i.p.) (B), ESM with SAIO nanoparticles (ESM_SAIO) (40 mg/kg, i.p.) (C), and ESM with temperature-sensitive SAIO nanoparticles (ESM_TSAIO) (40 mg/kg, i.p.) (D).

ESM had significant effect in reducing the number and total duration of spontaneous SWDs (Figure 8A). ESM_SAIO (Figure 8B) and ESM_TSAIO (Figure 2C) significantly decreased the number of total duration of spontaneous SWDs. The data support that ESM with nanoparticle synthetic process preserves its effect in SWD suppression. However, the dimension of the magnetic machine which induces heat becomes a major problem to design a close-loop small-size seizure controller. An electric inductor made of MEMS technique is now developed. **This infusion chamber had ability to push ESM_SAIO into the brain and obtained a significant reduction of SWD number with a dose-dependent manner (Please refer SubProject II).**

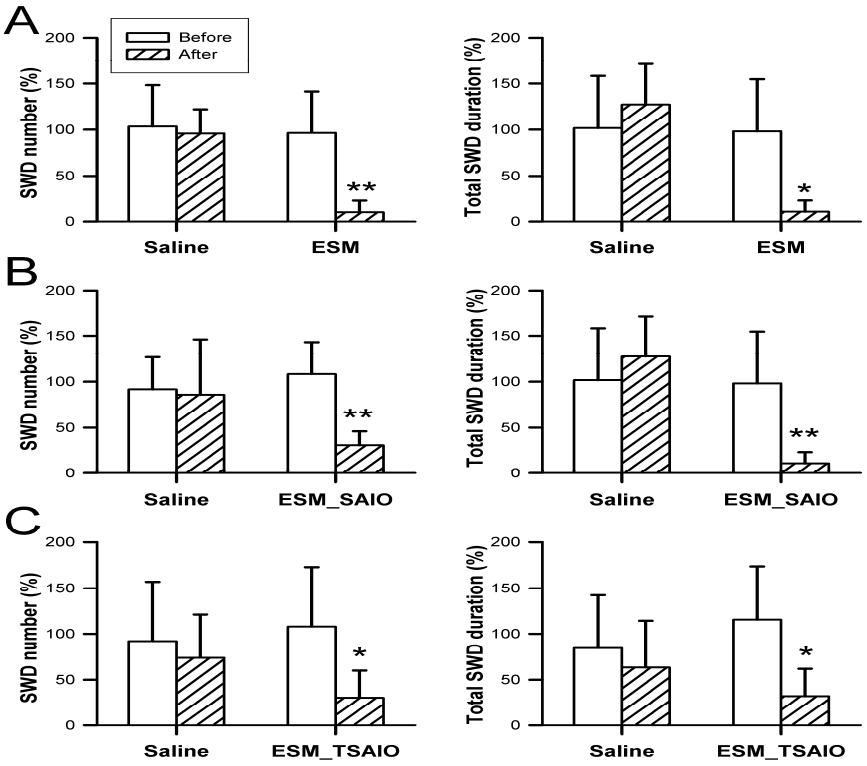

Figure 8. Comparison of SWD number and total SWD duration with saline and 3 different forms of ESM in Long-Evans rats with spontaneous SWDs (n = 8). (A) ESM (0.5 ml, 28 mg/kg, i.p.) significantly decreased SWD number and total SWD duration. (B) ESM with SAIO nanoparticles (ESM_SAIO) (40 mg/kg, i.p.) significantly reduced SWD number and total SWD duration. (C) ESM with temperature-sensitive SAIO nanoparticles (ESM_TSAIO) (40 mg/kg, i.p.) significantly reduced SWD number

and total SWD duration. * $P < 0.01$; ** $P < 0.001$ by paired *t* test.

P-2. Effects of intracortical ESM infusion in spontaneous SWDs

Animal preparation was similar to experiment 1. Additionally, stainless steel canulae were bilaterally inserted into lateral (LSC) or medial somatosensory cortices (MSC) (A0L5, anterior 0 mm lateral 5 mm; A0L2, anterior 0 mm lateral 2 mm with regard to the bregma) to delivery saline or ESM. One-hour spontaneous brain activity was recorded as baseline. Saline or ESM of 2 μl was progressively infused in 5 minutes, and afterwards 1-hour recording was made. Several aspects of SWD results about intracortical microinfusion of saline and ESM (200 nmole) into 3 brain sites were evaluated

Figure 9A show a barrage of representative SWDs of Long-Evans rats. The SWDs were bilateral synchronization. Figure 4 depicts placements of infusion cannulas in the MSC and LSC. Infusion of ESM into the LSC region produced an immediate and substantial increase in SWD onset latency, decrease in SWD number and cumulative duration (Figure 10). Four out of 10 Long-Evans rats (40%) were free of SWDs 1 hour after ESM infusion into the LSC. In contrast, infusion of ESM into the MSC regions had no obvious effect in all indexes (Figure 11). In addition, bilateral infusion of saline into MSC or LSC regions of the Long-Evans rats showed no effect on SWD onset latency, SWD number, cumulative SWD duration, and mean SWD duration. The factor of cannula placement (LSC vs. MSC) was significant difference in SWD onset latency ($F_{1,18} = 6.476$, $P = 0.02$), cumulative SWD duration ($F_{1,18} = 5.48$, $P = 0.031$), and mean SWD duration ($F_{1,18} = 6.221$, $P = 0.023$). The treatment (ESM vs. saline) showed a significant effect in SWD onset latency ($F_{1,18} = 10.403$, $P = 0.005$), SWD number ($F_{1,18} = 4.973$, $P = 0.039$), and cumulative SWD duration ($F_{1,18} = 4.421$, $P = 0.049$). Interaction between the cannula placement and treatment was significant in SWD onset latency ($F_{1,1} = 5.225$, $P = 0.035$) and SWD number ($F_{1,1} = 8.034$, $P = 0.011$). In this study, bilateral infusion of ESM into the LSC significantly inhibited SWDs in terms of slowing onset latency of SWDs as well as decreasing SWD number and cumulative SWD duration in Long-Evans rats with spontaneous SWDs. The data will be very important and useful for the **central theme of the Project** in the development of a real-time, close-loop seizure controller.

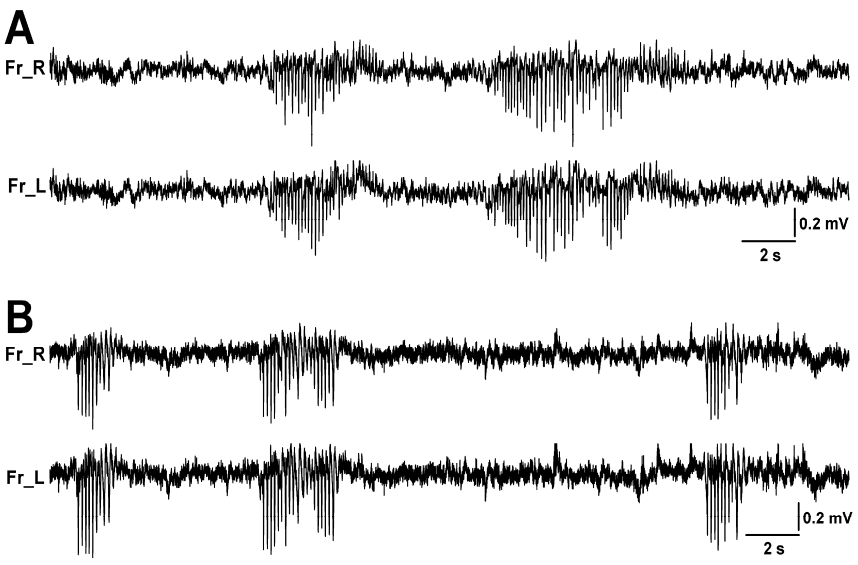

Figure 9. Representative examples of spontaneous SWDs (A) and pentylenetetrazol (PTZ)-induced SWDs (B). Temporal and spectral characteristics of spontaneous SWDs and PTZ-induced SWDs were very similar.

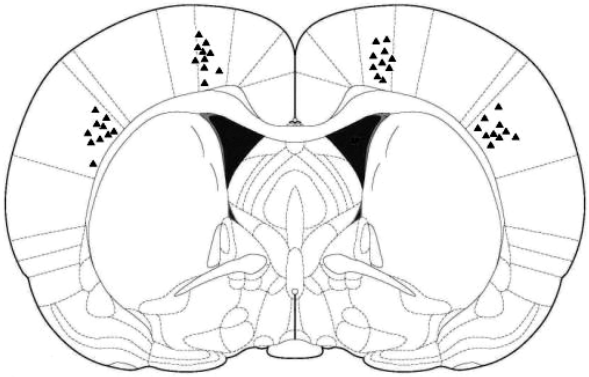

Fig. 10. Coronal brain sections of Long-Evans rats taken at 0.0 mm relative to bregma adapted from Paxinos and Watson 4th edition. Triangle symbols indicate infusion cannula placement.

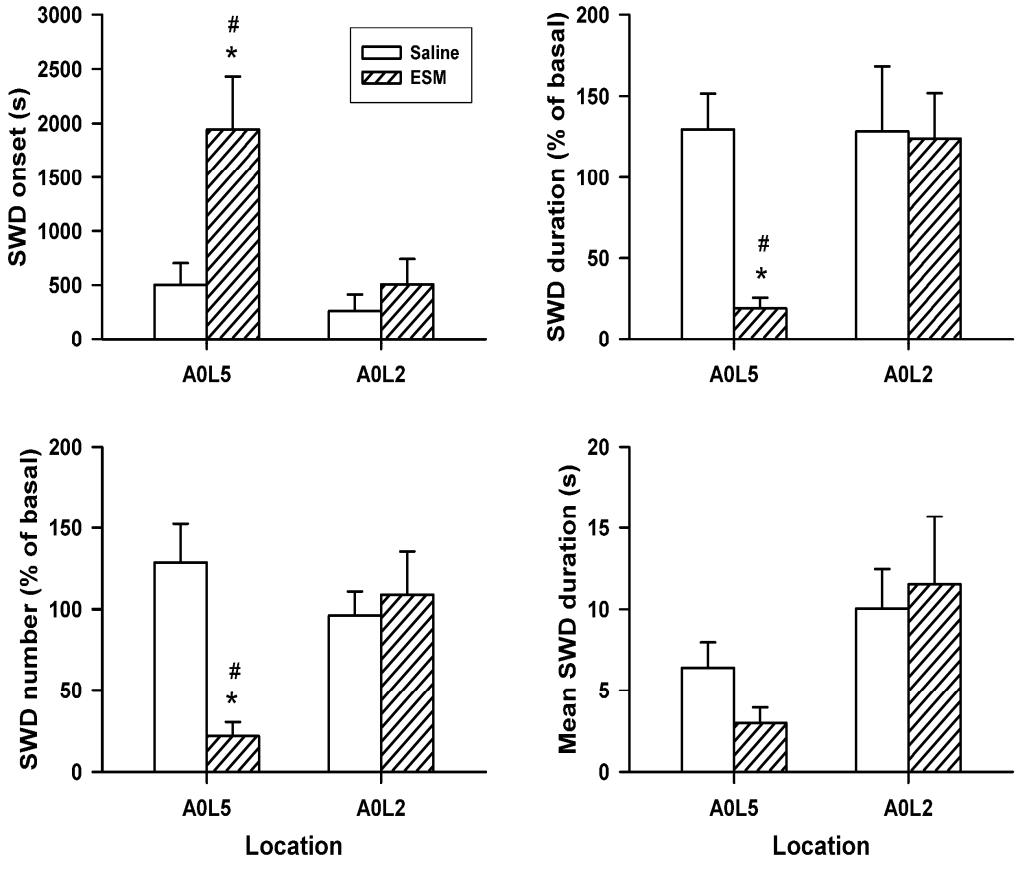

Fig. 11. Effect of saline and ESM microinfusion into the lateral somatosensory cortex (A0L5) and medial somatosensory cortex (A0L2) on SWD onset latency, SWD number, cumulative SWD duration, and mean SWD duration in Long-Evans rats. * $P < 0.05$ vs. saline of A0L5; # $P < 0.05$ vs. ESM of A0L2.

(3) Sub-Project-3:

Development of epilepsy platform for a novel real-time system for seizure detection and delivery of antiepileptic drug

In the present study, Long-Evans rats are used because they often display spontaneous SWDs, which have been demonstrated to be associated with absence seizures in several aspects of evidence. To confirm the cortical focus theory of SWDs, a pharmacological epileptic rat model, i.e., low-dose pentylenetetrazol (PTZ) (20 mg/kg, i.p.) in Wistar rats, was also used. Here, we performed three experiments: One was comparing effect of saline, ethosuximide (ESM), ESM with SAIO nanoparticles (ESM-SAIO) and ESM with temperature-sensitive SAIO nanoparticles (ESM_TSAIO) in spontaneous SWDs of Long-Evans rats. Second, comparison of effects of intracortical injection of saline and ESM into 3 different brain sites in spontaneous SWDs of Long-Evans rats. Third, effects of intracortical injection of saline and ESM into 3 different brain sites in PTZ-induced SWDs of Wistar rats were compared.

P-1: On-line and Real-time Seizure Detector

The responsive drug delivery system requires a robust on-line seizure detector so that the drug delivery device can be turned on as soon as possible when a seizure occurs. An on-line seizure detection method for responsive antiepileptic devices should satisfy the following requirements: 1) it should achieve a high seizure detection rate and low incidence of false alarms, 2) it should be easily implemented on a portable or implantable device, and 3) it should have high performance in on-line seizure detection of freely moving subjects.

To achieve these goals, EEG data corresponding to various behavioral states was utilized for model construction and evaluation in this study. Approximate entropy and power spectrum of EEG signals with respect to various physiological states were integrated as the features. A linear classifier called linear least square (LLS) method was utilized to detect the seizure events and to reduce the computational cost for practical implementation on embedded or hardware systems (Liang et al, 2009, 2010a). Thereafter, a temporal constraint and an adaptive thresholding mechanism were also proposed to reduce the false detection rate during the

grooming or wake-sleep states.

In our experiment, it was observed that most of the false detections occurred in the grooming and the slow wave sleep (SWS) state for rats. To decrease the incidence of false alarms, an adaptive thresholding rule is proposed to switch the threshold of the LLS. Because the SWS of rats has a high-amplitude oscillation within delta frequency range (0.5-4 Hz) and that high energy in low frequency band also appears in grooming. If the averaged power level of the frequency band during the delta band was higher than a predefined constant value, the threshold of the LLS was switched to a higher value to reduce the false detection rate. Figure 12 shows the block diagram of the proposed seizure detection method.

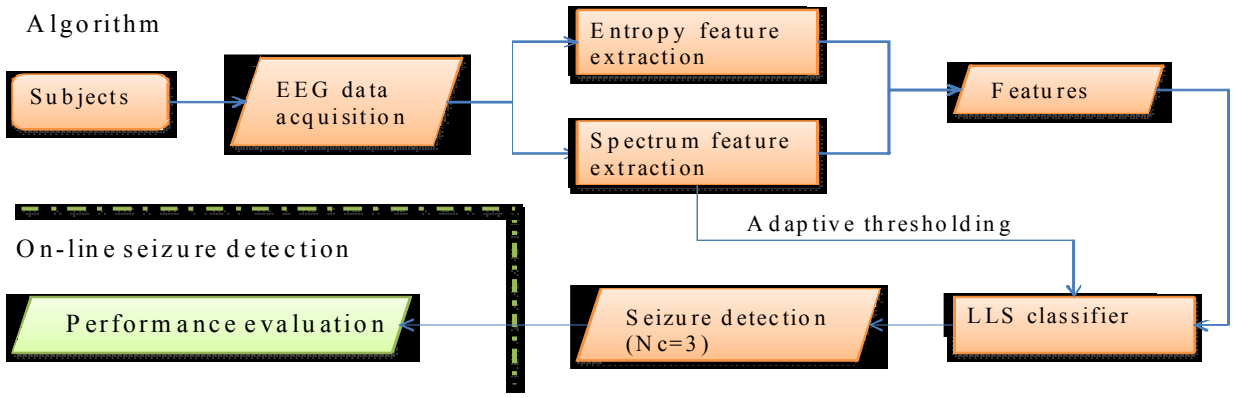

Fig. 12. Block diagram of the proposed seizure detection method.

In order to develop a portable seizure detector, the developed method has been implemented on an embedded system to perform on-line seizure detection (Young et al, 2010; Liang et al, 2010b). The schematic diagram of the on-line seizure detection system is shown in Fig 13. This system contains four units: (a) a signal acquisition and amplification unit, (b) a signal processing unit, (c) a wireless data transmission unit, and (d) a host system for on-line monitoring, warning and storage. The signal acquisition and amplification unit is applied to measure the EEG signal in the frontal cortex of the rat. The spontaneous EEG was amplified 1000 times and bandpass filtered between 0.8 Hz and 72 Hz. The Texas Instrument (TI) CC2430 embedded analog-to-digital converter (ADC), a ZigBee transceiver, and an 8051 microcontroller unit (MCU) was utilized to perform sampling, signal processing and transmission tasks. The resolution of the ADC was configured to 10 bits and the sampling rate was 200 Hz. The developed seizure detection method was implemented on the MCU to perform real-time operation. For the monitoring host, a TI SmartRF04 Evaluation Board with a CC 2430 module was used for receiving the EEG signals and the seizure detection sequence (0 or 1). A graphic user interface (GUI) was developed and operated on a laptop for data display/storage and auditory feedback for seizure warning.

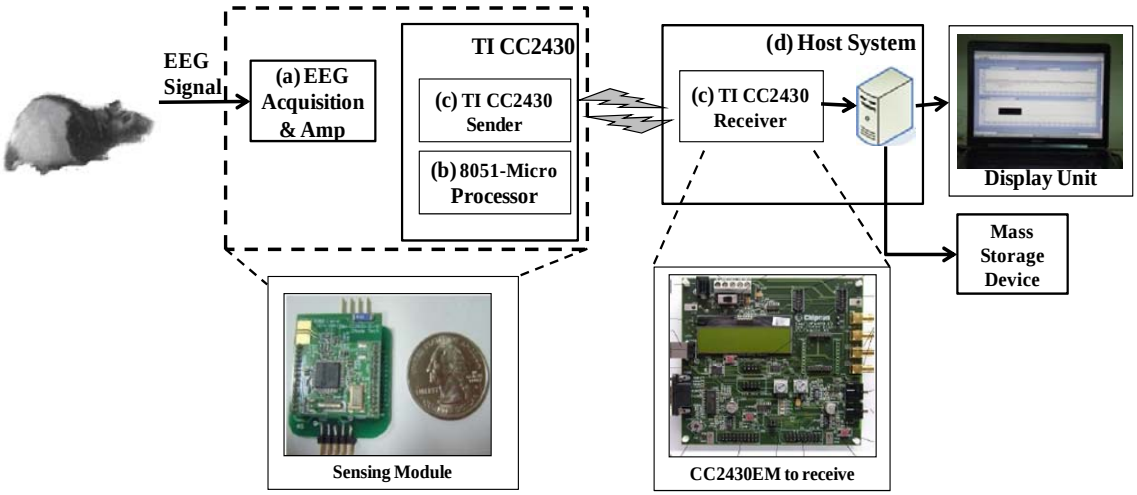

Fig. 13. Schematic diagrams of the developed portable seizure detector.

P-2. The Wireless Multi-Channel Behavioral State Monitoring System

In order to monitor the spontaneous convulsive epilepsy such as the Kindling rat model, it is critical to set up a precise and feasible monitoring system. In this study, a behavioral state and physiological signal monitoring system was also developed for the monitoring of the Kindling process (Chang et al, 2010). Four EEG and three-axis accelerometer signals are acquired and transmitted to a host computer for further automatic analysis or visual review. The wireless communication based on IEEE 802.15.4/ZigBee frees the experimental subject from the hassle of wires and reduces the wire artifact of EEG signal during convulsions. This system features low cost, compact size, low power, and real time by eliminating video, EMG and EOG installation and detection. It demonstrates successful discrimination of vigilance states, while a long period of recording is also verified.

This monitoring system is composed of a data acquisition device carried by each experimental subject for acquiring the EEG and accelerometer signals, and a near-by host computer configured as a virtual instrument (VI) for remote real-time physiological signal and behavioral state monitoring, while they communicate each other based on a 2.4 GHz wireless IEEE 802.15.4/ZigBee protocol. The host computer, which is originally not capable of IEEE 802.15.4 communication, utilizes RS-232 to connect with a Texas Instrument SmartRF04 Evaluation Board with a CC2430 Evaluation Module for EEG and accelerometer data reception. Table 1 shows dimension, weight and current consumption of the wireless multi-channel data acquisition system.

The developed system has been mounted on the freely moving rats to perform various behavioral state and physiological signal monitoring experiments for demonstration. Figure 14 demonstrates a rat being able to carry the data acquisition device without wire hassle and motion constraint. The accelerometer board was mounted on the head of a rat while the other

boards together with the battery were mounted on a jacket worn by the rat. The axis of the accelerometer with respect to a rat's head is illustrated in Fig. 15. The X, Y and Z axes direct to the front-rear, up-down, and left-right directions, respectively. One to four EEG channels at frontal cortex and/or amygdale were simultaneously recorded depends on different experimental settings. The video recording was also performed during the experiments to confirm the behavioral states of the rats.

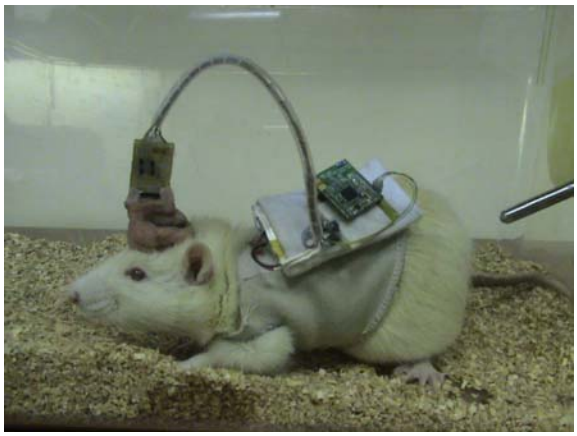

Fig. 14. The developed wireless multi-channel behavioral state monitoring system installed on a rat.

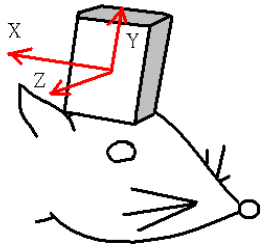

Fig. 15. Placement of the 3 axis accelerometer with respect to the rat's head for the developed multi-channel behavioral state monitoring system. The X, Y and Z axes direct to the front-rear, up-down, and left-right directions, respectively

TABLE 3. DIMENSION, WEIGHT AND CURRENT CONSUMPTION OF THE DATA ACQUISITION SYSTEM

	Accelerometer board	**EEG amplification board**	**Microcontroller board**
Dimension (mm×mm×mm)	25 × 17 × 5	34 × 30 × 6	24 × 27 × 8
Weight (g)	0.96	2.75	2.25

Average Current Consumption (mA)	19.6
Battery Life (hour)	56 (3.7V, 1100 mAH)
Battery weight (g)	17.98

P-3: The Electrically-responsive Drug Delivery Device with the Automatic Seizure Detector

The developed seizure detector was also integrated with the drug delivery device developed in subproject 2 to perform a responsive drug delivery system and this system was evaluated by the rat models developed in subproject 3. In our preliminary in-vivo study, a unique design by integrating the biological self-detection and response-induced features of the chip on epileptic treatment was demonstrated. The architecture of the whole drug delivery system is shown in Fig. 16. The drug delivery system consists of four units: (a) signal acquisition and amplification unit, (b) 8051 micro-processor and wireless data transmission unit, (c) electric field and drug delivery chip, (d) host system for data storage and real-time display.

It can be observed in Fig. 16(a) that electroencephalogram (EEG) signal of the rat's frontal cortex is amplified and band-pass filtered (1000x, 0.3-80 Hz) by the op-amp, and then the amplified EEG is positive-biased to the input voltage range of an analog-to-digital converter (ADC) (Texas Instrument CC2430 chip). Thus, several tasks were implemented on the microcontroller board (MCU) (refer to Fig. 16(b)), including analog-to-digital conversion of EEG signals, execution of seizure detection, generation of trigger to the drug releasing chip, and EEG data wireless transmission. The MCU was programmed to control the sampling period of the ADC and the generation of trigger, retrieved the direct memory access (DMA) data, and started a series of feature extraction and seizure detection. The system detected epileptic seizures and immediately feedbacks to stimulate electric at the drug releasing chip (refer to Fig. 5(c)) to induce drug elution. Electric filed activated the structural change of the hybrid hydrogel in the chip to release drugs accordingly. Therefore, the controlled release system is regarded as a closed-loop drug delivery system on epilepsy control, as shown in Fig. 16(a)-(c). Furthermore, in order to achieve real-time monitoring, the real-time on-line seizure monitoring was developed using National Instrument LabVIEW to create a graphical user interface (GUI) VI to monitor and store the EEG data(refer to Fig. 16(d)).

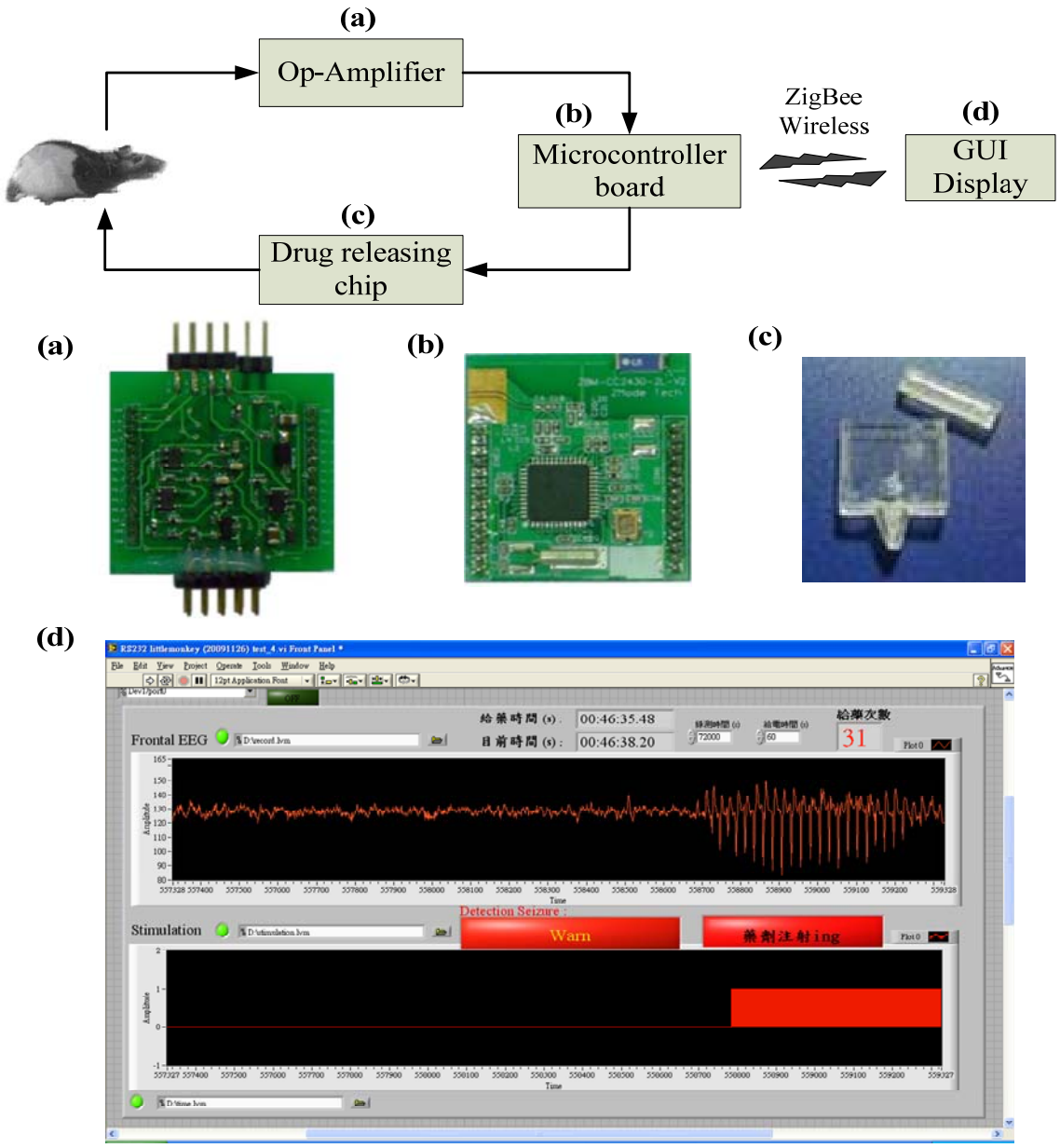

Fig. 16. Schematic illustration of the electrically-responsive drug delivery system. (a) signal acquisition and amplification unit, (b) 8051 micro-processor and wireless data transmission unit, (c) drug releasing chip, (d) host system for data storage and real-time display.

A complete view of the backpack and of its placement on a rat is given in Fig. 17(a). There are two batteries in the backpack. In order to minimize the weight of head mounted devices for a rat, the backpack was mounted on the rat's jacket which was connected to the neural interface by short soft wires. Generally, the shorter the wires, the lower the noise picked from the environment. The detailed caption was given in Fig. 17(b), the neural interface consists of op-amplifier and constant voltage circuits. On the other hand, the microcontroller board used Texas Instrument CC2430 chip to compute detection epileptic seizure. When the MCU detects

epileptic seizures, it would feedback immediately to trigger chip to release drug into the rat during eight minutes. The funnel chip can be demonstrated in the inset of Fig. 16(c).

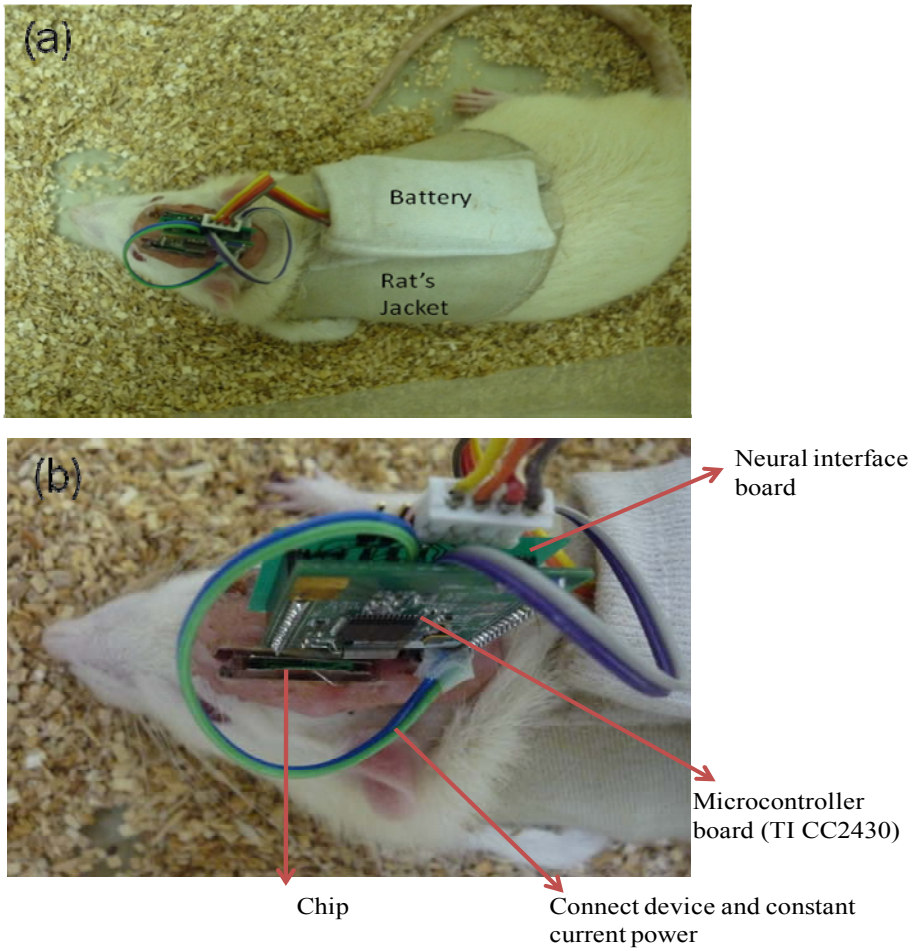

Fig. 17. Experimental setup of the animal study and the illustration of the drug release system, where the "chip" indicates the drug delivery device.

A 40-minutes spontaneous brain activity during released process and 20-minutes spontaneous brain activity after treatment was analyzed. Figure 18 demonstrates that the SWD of the rats reached ~120 times without drug administration while the SWD of the rats reduced by nearly 50% while ESM was released from the self-detection drug delivery system. Although it is hard to quantify the exact amount of the ESM release into the rats during the in-vivo operation, it is truly indicated that certain effective dose of ESM was released into the rats from the chip-based drug delivery system, which, for the first time, proved the concept of the integrated system designed based on the electrical-responsive hybrid hydrogel. Although this in vivo study has far from being optimized in terms of operation parameters among different parts of the integral system, drug dose, and time of dosing, the preliminary in-vivo outcomes do provide promising perspective toward further investigation. It is highly expected by combing photolithography technology frequently employed in semi-conductor industry, the implantation of the chip-based

system would be expected to offer self-detection and effective therapeutic treatment for epileptic patients, and those who suffers from chronic diseases, in the future.

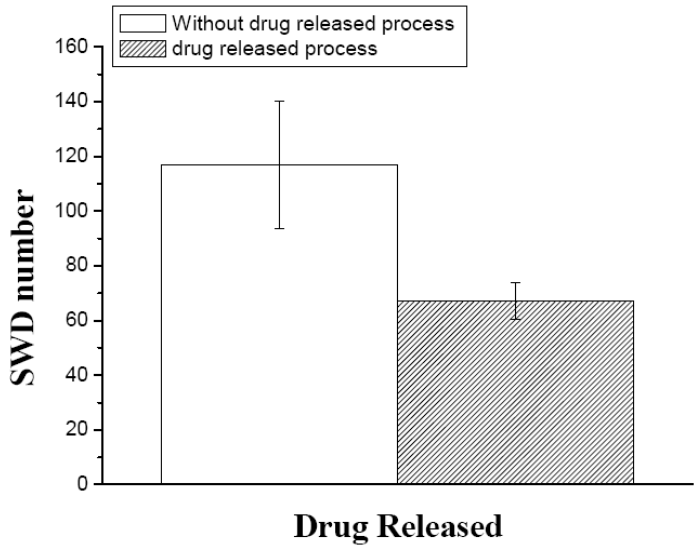

Fig. 18. Comparison of SWD number of the rats (n=6) with and without (as control group) drug elution from the chip-based drug delivery system.

四、Achievements (執行成果績效)

1. 本子計畫符合執行進度。

2. 對於團隊間研究資料分享與配合為優。本計畫不僅提供**子計畫二**奈米藥物之動物測試平台，亦提供**子計畫一**自發性失神癲癇大鼠腦波以及 Amygdala 誘發之顳葉抽搐型癲癇之腦電波訊號。目前本計畫已進行電場式的奈米型 ESM 灌流裝置並完成初步實驗測試，已經發現在側邊大腦區域灌流奈米型 ESM 可以顯著地抑制失神性癲癇放電次數，其抑制效果並與劑量成正相關，此結果支持本計畫之初步假說。相信未來的密閉式回授藥物型癲癇抑制器將可以進行實際的大量動物測試，以做為人體臨床測試前之重要資料庫。

3. Published papers and conference proceeding:

Chen S.-D., Yeh K.-H., Huang Y.-H., **Shaw F.-Z.*** (2010) Effects of intracortical administration of ethosuximide in rats with spontaneous or pentylenetetrazol-induced spike-wave discharges. Epilepsia, in revision. (IF: 4.052) (SCI)
Lee H.-W., Huang H.-Y., Chen S.-D., **Shaw F.-Z.*** (2010) Chronic lamotrigine treatment on a rat model with spontaneous spike-wave discharges. Epilepsia, in submission. (IF: 4.052) (SCI)

Liang SF, Chang WL, Liao YC, Chen YJ, Wang HC, **Shaw FZ**. (2010) On-line real-time seizure detection in rats with spontaneous absence or pentylenetetrazol-induced epilepsy. Journal of Neural Engineering, in submission. (IF: 3.739) (SCI)
Shaw FZ*, Liao YF, Chen RF, Lin RCS. The zona incerta in spontaneous spike-wave discharges of the rat. *Cerebral Cortex*, in preparation. (impact factor: 5.907) (SCI)
Shaw FZ, Huang CC. "Distortionless powerline interference removal method using S-transform" 中華民國專利 97133429.
Liao YC, Hsieh CH, Liang SF, Young CP, Chang DW, **Shaw FZ**. A Wireless and Portable Real-time Epilepsy Detection and Control System. Biomedical Engineering Society 2009 Annual Symposium (2009 生物醫學工程年會及科技研討會), Taipei, Taiwan (2009).[學生口頭論文競賽佳作]
Shaw F.-Z.* (2010) Epileptic rat models for a closed-loop seizure controller. Annual Meeting of Taiwan Epilepsy Society, Taipei, Taiwan.
Shaw F.-Z.* (2010) Epileptic rat models for a closed-loop seizure controller. 4th Asian Epilepsy Surgery Congress, Taipei, Taiwan.
Shaw F.-Z.*, Yeh K.-H. (2010) Lateral somatosensory cortex in spontaneous and PTZ-induced spike-wave discharges of the rat evaluated by ethosuximide. 16th World Congress of Basic and Clinical Pharmacology, Copenhagen, Denmark.
Liang S.-F., **Shaw F.-Z.**, Young C.-P., Chang D.-W., Liao Y.-C. (2010) A closed-loop brain computer interface for real-time seizure detection and control. 32nd Annual International IEEE EMBS conference, Buenos Aires, Argentina.
Lee H.-W., Huang H.-Y., **Shaw F.-Z.*** (2010) Chronic lamotrigine treatment on seizure and anxiety-/depression-like behaviors of the rat with spontaneous absence epilepsy. 49th Annual Conference of Taiwanese Psychology Association, Chiayi, Taiwan.
Yen-Po Chang, Kun-Ho Liu, Chih-Shin Chao, **San-Yuan Chen***, Dean-Mo Liu, Synthesis and characterization of mesoporous Gd2O3 nanotube and its use as a drug-carrying vehicle, **Acta Biomaterialia** 6 (2010) 3713–3719. (**IF=3.98**, N/M=5.1%)
Shang-Hsiu Hu, Kuan-Ting Kuo, Wei-Lin Tung, Dean-Mo Liu,and **San-Yuan Chen*** , A Multifunctional Nanodevice Capable of Imaging, Magnetically Controlling, and In Situ Monitoring Drug Release, **Advanced Functional Materials**, 19, 3396–3403 **(2009)** (IF=6.99, N/M=4.21%)
Wei-Chen Huang, Kun-Ho Liu, Shang-Hsiu Hu, **San-Yuan Chen*** and Dean-Mo Liu, "A Flexible Drug Delivery Chip for Magnetically-Controlled Release of Anti-Epileptic Drug", **Journal of Controlled Release 139 (3), 221-228, NOV (2009)** (IF=5.949, N/M=5.90%)
C. P. Young, S. F. Liang, D. W. Chang, Y. C. Liao, F. Z. Shaw and C. H. Hsieh, "A Portable Wireless On-line Closed-loop Seizure Controller in Freely Moving Rats," IEEE Trans. on Instrumentation & Measurement, vol.59, No. 10, in press, 2010.
S. F. Liang, H. C. Wang, W. L. Chang, " Combination of EEG Complexity and Spectral Analysis for Epilepsy Diagnosis and Seizure Detection," EURASIP Journal on Advances

Signal Processing, vol. 2010, 853434, 15 pages, 2010a.
S. F. Liang, F. Z. Shaw, C. P. Young, D. W. Chang, and Y. C. Liao, “A closed-loop brain computer interface for real-time seizure detection and control,” *32rd Annual International Conference of the IEEE Engineering in Medicine and Biology Society*, 4950-4953, Buenos Aires, Argentina, Aug. 31 – Sep. 4, 2010b
S. F. Liang, W. L. Chang, and H. M. Chiueh, “EEG-based Absence Seizure Detection Methods,” in *Proceeding of International Joint Conference on Neural Networks 10*, Barcelona, Spain, July, 1725-1728, 2010c.
D. W. Chang, S. F. Liang, C. P. Young, F. Z. Shaw, Y. D. Liu, Y. C. Liu and J. J. Chen, "A Wireless Portable Behavioral State and Physiological Signal Monitoring System for Freely Moving Rats", in *Proc. Int. Instrum. Meas. Technol. Conf.*, Austin, pp. 1353-1357, 2010.

4. Patent:

1. **Shaw FZ**, Huang CC. “Distortionless powerline interference removal method using S-transform” 中華民國專利 97133429.

2. 應用於慢性疾病的生物自我偵測及回饋誘導藥物釋放系統
申 請 日：民國 99 年 9 月 15 日
申請國家：中華民國、美國
案件類型：發明

智慧型生物訊號誘導藥物釋放系統前瞻研究:以癲癇症為模式－應用於訊號誘導藥物釋放系統之智慧型生醫複合材料結構製程與性質研究(子計畫二)

Frontier Research on Smart Biologically-Stimuli Drug Delivery System Based on Epilepsy - Development and characterization of smart responsive biomedical composite structure for drug delivery system

計畫編號：NSC-98-2627-B-009-001
執行期限：98年8月1日至99年7月31日
主持人：陳三元　　國立交通大學材料科學與工程學系
共同主持人：黃國華　　國立交通大學奈米科技研究所

一、 中文摘要

本子計畫的最主要目標在於開發一個可應用於癲癇症之智慧型生醫複合材料結構製程,並與子計畫-1及子計畫-3整合發展成一個具有迴饋偵測及治療。當偵測到癲癇異常放電時，啟動藥物釋放系統給藥以抑制異常放電的電刺激之藥物載體結構。因此本計畫在第三年度主要是發展一個以兩性幾丁聚醣和無機二氧化矽為材料的生物相容複合水膠，其組成、熱穩定性和結構都會被分析與最佳化。以抗痙攣藥物-乙琥胺為模擬藥物，電敏感複合水膠在體外試驗呈現系統化的釋藥行為。其釋藥行為是由於在直流電場下，藥物分子和複合水膠電特性被電泳機制和電滲行為影響產生。經由癲癇老鼠模型更進一步的調察發現，被設計成系統化的貯藥體,複合水膠,能夠自行偵測與傳遞訊號,使老鼠的癲癇發作次數降低。經由這計畫的整合研究的確已經可以達到當初的目標,希望未可以在實際癲癇療程證明其自行偵測和系統化藥物傳輸的特性。

關鍵詞：電敏感性、奈米結構混層水膠、藥物載體、藥物釋放傳遞、自我偵測迴饋、癲癇

Abstract

This study reports the development of a biocompatable Nano-structured hybrid hydrogel based on an amphiphilic chitosan and inorganic silica, where the chemical composition, thermal stability and structural integrity of the resulting hybrid were characterized and optimized. Electrically-responsive drug elution behavior of the hybrid hydrogel was evaluated systematically in-vitro using an anticonvulsant drug, ethosuximide, as model molecule. The release behavior was explained using a combined mechanism of electrophoretic and electro-osmotic actions between drug molecule and electron mobility of the hybrid hydrogel under a given DC electric field. Further integrating the hybrid hydrogel, designed as a chip-like drug reservoir, with an automatic self-detection and signal transmitter system, applying to a rat's model, the resulting seizure frequency was considerably reduced and has experimentally proved that such a self-detection chip-like drug delivery device holds promising prospective in practical epileptic treatment.

Keywords: Electrically-responsive, Nanostructured Hybrid hydrogel, Controlled drug release, Drug delivery device, Self-detection and Feed-back, Epilepsy

二、緣由與目的

The average life span of human has been prolonged considerably due to the explosive development of medical science and technology over recent decades, where advanced therapeutic strategies have been extensively explored and collectively employed to various disease treatments. Up to date, efforts to efficiently deliver therapeutic drugs to patients with minimal side effects, enhanced efficacy and improved compliance have received greatest attention worldwide in recent decade. Among the development of drug delivery systems, demands for biological self-detection and response-induced features of drug delivery system has been most interesting and is foreseeing its future market development due to increased amount of aged population [1]. Therefore, combination with an intelligent rapid response drug delivery system is the trend for biotechnology and medical technology. A multi-functionalized drug delivery nanosystem would be required and designed, including targeted mechanism, diagnosis and real-time controlled drug release.

Drug delivery systems can be controlled by applying an external stimulus included electrical field, magnetic field and ultrasonic waves, etc, upon which drug is eluted with a pre-designed pattern from the system to diseased host to minimize life-threatened occurrence [2-5]. However, each part of the therapeutic treatment is operated discretely, with no relevant signal intimately connected separate parts and this renders possible lose of best time of medication. Therefore, it needs to develop a drug delivery system by combination of wireless detector, close-loop automatic detection system and response-induced drug release system [6,7].

Under ideal operation, it is expected that through amplifier and wireless signal transition, the systems can simultaneously diagnose whether the symptom has occurred. Then, the drug-content device elutes drug with therapeutically effective dose based on detection and translation of the corresponding intensity of abnormal signal by the system. Through such an operation, it would reduce the side effects on the patients. Epilepsy, for example, can be detected by analyzing the electroencephalogram (EEG) data, and can be employed as a disease model for study and was used in this work [8-11]. To design a system for analyzing EEG data, the signal induced by the system can feedback to manipulate drug release with a signal-dose dependent manner. Thus a system, consists of signal amplifier, wireless transmitter, and drug delivery device, can be a very useful clinical tool for epilepsy treatment. The former two components have been successfully developed and tested in a number of earlier studies [12-14], and it turns to be more critical to develop a drug delivery system which can be smartly responding to the signal translated from the system, giving a timely and effective medical treatment and this is one of the major research objective of this work, where a smart and mechanically reliable hybrid hydrogel is designed and developed for the purpose.

Use of an environmentally responsive hydrogel as reservoir to deliver therapeutic substances has received widest attention for recent decade [15,16]. However, mechanical fatigue and weakness of polymeric hydrogels renders a long-term application more challenged, for instance, structural collapse or degradation of a given hydrogel under cyclically environmentally-induced (mostly, electric field) mechanical deformation may occur. Relaxation of the deformed hydrogel when removed the induced field may also retard the efficiency of the subsequent release of the drug, reducing therapeutic efficacy to a certain extent, this is especially critical for acute symptom such as epileptic seizure. Increasing addition of chemical cross-linker may achieve better performance, however, deteriorating biocompatibility of the resulting hydrogels. Therefore, to reinforce the conventional hydrogels with improved responsiveness and cyclic service performance to the external stimulus, an attempt of incorporating higher inorganic component together with a minimal concentration of organic cross-linker was made in order to ascertain the biocompatibility of resulting hydrogels and improved stimulus-induced responsiveness. In this work, a modified chitosan was employed, which was characterized with biocompatibility, biodegradability, non-toxic, non-irritable, and moisturized as described in our previous

publications[17,18]. This modified chitosan was further hybridized with inorganic silica and a cross-linking agent. The resulting hybrid hydrogels were characterized and employed as a drug reservoir for electrically-response drug delivery system in vitro. Further integration to form a biological self-detection and signal conversion system to deliver anti-epileptic drug in vivo was demonstrated where the instantaneous epileptic discharge can be detected through the signal conversion into electric, and these signals will activate the structural change of the hybrid hydrogel to trigger drug elution through wireless transmission.

2. Experimental Procedures

2-1 Synthesis of CHC

The synthesis of carboxymethyl-hexanoyl chitosan (CHC) has been detailed in our previous report[17], Briefly, 5 g of chitosan was suspended in 2-propanol (50 mL) at room temperature while being stirred for 30 min. The resulting suspension was gently mixed with 12.5 mL NaOH solution. The mixture containing NaOH of 13.3M was mixed with 25 g of chloroacetic acid to prepare carboxymethyl chitosan sample with a high degree of carboxymethyl substitution. Obtained and dried sample (2g) was dissolved in distilled water (50 mL) while being stirred for 24 h. These resulting solutions were mixed with methanol (50 mL), followed by the addition of hexanoyl anhydride at a concentration of 0.5M for the CHC samples with the degree of carboxymethyl and hexanoyl substitution of 0.50 and 0.48, respectively. After 12-h reaction, the resulting solutions were collected by dialysis membrane (Sigma Chemical Company, USA) using ethanol solution (25% v/v) for 24 h. The chemical structure of the CHC is shown in Fig. 1 where the sites and degrees of substitution were quantitatively confirmed by ^{1}H NMR analysis [19].

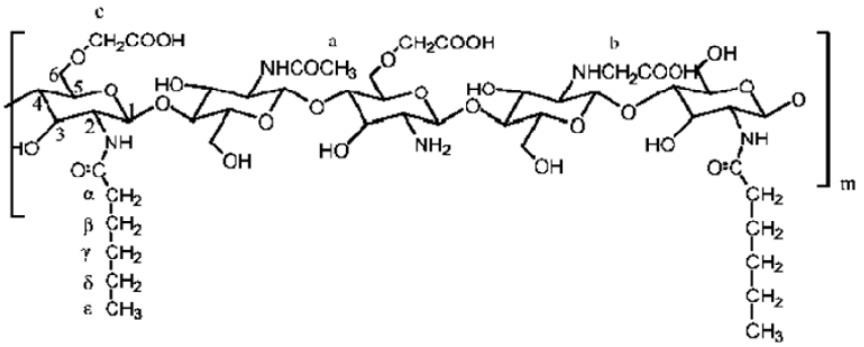

Fig. 1. Chemical structure of CHC

2-2 Preparation of CHC Hydrogels

To prepare CHC hydrogels, the preparation procedure is separated into two stages, the first stage is to prepare three suspensions; (1) 1.3% w/v CHC solution by suspending the above-mentioned CHC samples in deionized water at 25 ^{o}C for 24 hours. (2) 1% w/v GP (genipin, Challenge Bioproducts Co., Ltd., Taiwan) solution which is prepared by dissolving GP powders in deionized water stirring for 2 hours at 50^{o}C to ensure that GP was fully dissolved, and (3) acid-hydrolyzed TEOS solution by mixing TEOS, together with ethanol and H_2O with different weight ratios ([TEOS]:[H2O]:[Ethanol]=1:5:7, 2:5:7, and 1:10:14 separately), and HCl, in order to give a final silica-containing CHC hybrid structure. After that, the GP and TEOS solutions with different weight ratios were added to the CHC solution while stirring for 30 minutes, followed by incubating at 50^{o}C for 2 days. Thus, the genipin-cross-linked CHC-TEOS hybrid hydrogels were formed and designated as GP*x*TEOS*y*, where the symbol *x* and *y* represent the weight ratios (in percentage) in the dried hydrogel. The synthetic parameters of hybrid hydrogels are listed in Table 1.

Table 1. The synthesis parameters of CHC-TEOS hydrogels designated as GP*x*TEOS*y*, where the symbol *x* and *y* represent the weight ratio in the dried hydrogel.

CHC Hydrogel	1.3 % w/v $CHC_{(sol)}$(g)	1% w/v $GP_{(sol)}$(g)	TEOS (g)
GP0TEOS54	2	0	0.03
GP0.5TEOS54	2	0.03	0.03
GP1TEOS54	2	0.06	0.03
GP1.5TEOS54	2	0.12	0.03
GP1.5TEOS0	2	0.12	0
GP1.5TEOS27	2	0.12	0.018
GP1.5TEOS54	2	0.12	0.03
GP1.5TEOS70	2	0.12	0.045

2-3 Characterization

The hybrid hydrogel membrane was obtained via casting and drying the final solution mixture at 50°C in a petri-dish with a size of 3.0 cm in diameter. The average thickness and the average weight of the obtained dried membrane were about 0.10 mm and 0.3 g, respectively.

The appearance and morphology of the hybrid hydrogels were examined by using optical microscopy and scanning electron microscopy (S6700, JEOL, Japan) respectively. Samples, named as GP0TEOS54, GP0.5TEOS54, GP1TEOS54, and GP1.5TEOS54, were characterized by UV spectroscopy (Evolution 300, UV-Vis), where the resulting spectra show different absorption wavelength representing a variation in cross-linked density. Moreover, the dynamic weight loss test for those samples, i.e., GP1.5TEOS0, GP1.5TEOS27, GP1.5TEOS54, and GP1.5TEOS70, was conducted through a DuPont 2050 thermogravimetric analyzer which in the meantime is able to investigate the degree of interweaving of the silica phase against CHC phase. All tests were conducted in a flowing N_2 atmosphere (25 ml/min) using sample of 3~5 mg in weight over a temperature range 30^{o}C to 500^{o}C at a scan rate of 10^{o}C/min.

In order to measure the swelling ratio, each sample was weighed before and after immersion in phosphate buffer solution. After the excessive surface water was removed with filter paper, the weight of swollen samples was measured at a 5-min interval. The procedure was repeated five times, until no further weight gain was detected. The swelling ratio was determined according to the following equation:

$$\text{Swelling Ratio (\%)} = [(W_s - W_d)/W_d] \times 100$$

where W_s and W_d represent the weight of swollen and dried samples, respectively. All results are obtained by averaging of five measurements. The measurement error is estimated to be <3%.

2-4 Assembly of the Drug Delivery Device

The drug delivery device is designed by combination of hybrid hydrogels and a transparent, plastic container. Fig. 2(a) is a schematic flowchart which demonstrates the procedures to prepare the device. A transparent plastic container, made of poly (methyl methacrylic acid) (PMMA, YEONG-SHIN Co., LTD, Taiwan) has dimensions of 2cm x 2cm x 0.2cm with a single small opening of 0.2 mm in diameter on one side of the container, whilst the other three sides were mechanically sealed the PMMA plates. The one with the small opening is designed as the outlet for drug elution. Two rectangle-shaped platinum plate (Pt, YEONG-SHIN Co., LTD, Taiwan, 4cm x2cm x 0.1mm in dimension) were placed in a constant distance with two parallel sides of the acrylic container as electrodes. After the hybrid hydrogels was inserted into the container described above and sealed, a chip-like device was successfully produced (Figs. 2(a) and (b))

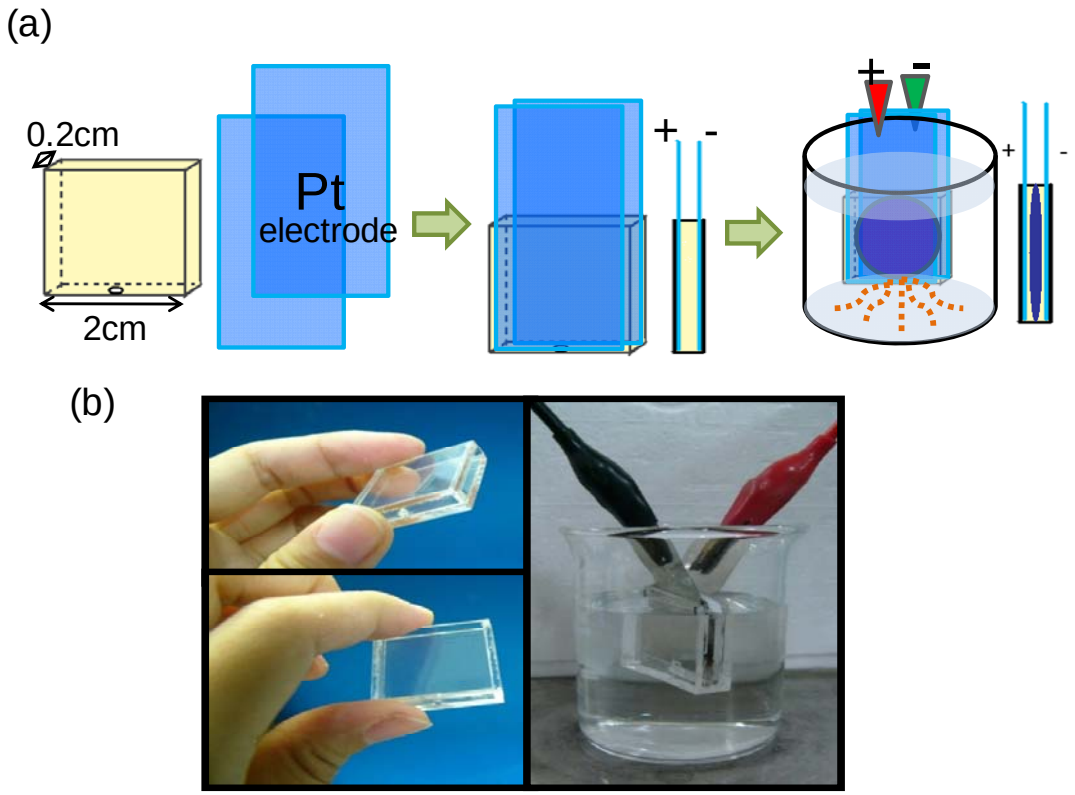

Fig. 2. (a) Schematic flowchart for chip-based hybrid device preparation (b) The setup of hybrid device where an electrical field of different strengths can be generated between the Pt electrodes in the sealed container.

2-5 Drug Release under Electrical Stimulation

Drug release test was carried out by first incorporating the hydrophilic anticonvulsant drug, ethosuximide (ESM), of concentration 15mg/ml, into the CHC solutions. The drug was dissolved completely in the presence of CHC-containing solution with a concentration of 1.5 wt%. Then after vigorously stirring, the final ESM-containing solution was cast in a petri dish and dried in oven at 50^{o}C to form resulting membrane-like hydrogels according to the preparative procedures aforementioned.

The ESM-loaded hybrid hydrogel with dimensions of 30 mm in diameter and 0.3 mm in thickness, on a dried basis, was kept in space between two platinum electrodes. Then, together with the final device, immersed into a glass beaker contained 50-ml distilled water. The device was then exposed under an electric voltage generated by a dc power source over a range of 0V, 15V, 30V, and 60V. At appropriate time intervals, 2 ml solution was extracted from the beaker and analyzed using a UV spectrophotometer (Evolution 300) at a specific wavelength λ=254 nm.

2.6 In-Vivo study

Adult Wistar rats were used in the study. Animals were kept in a room with a 12:12-h light-dark cycle with food and water provided ad libitum. All surgical and experimental procedures were reviewed and approved by the Institutional Animal Care and Use Committee of National Cheng Kung University. EEG was recorded over the area of the frontal barrel cortex (A +2.0, L 2.0 with reference to the bregma[20].

A proconvulsant, PTZ (20 mg/kg, i.p.), was injected into Wistar rats to provoke convulsive spike-wave discharges (SWDs). These behaviors were followed by intensive head nodding and facial twitching behaviors accompanied by SWDs sustaining for three hours after PTZ injection. Detailed experimental and recording procedures were described previously[21]. The dosage of ethosuximide (ESM) has been demonstrated to effectively and significantly reduce spontaneous

SWD incidence in absence-like seizure rats [22]. The two drug delivery devices were implanted over the left and right brain area of the primary somatosensory cortex (SI) (A 0.0, L ±5.0).

2.7 *Hardware*

We have successfully integrated electrical circuit and SOC (system-on-a-chip) technology, brain signal and real-time computing to develop the biological self-detection and response-induced features of drug delivery system on epilepsy. The drug delivery system is carried by each experimental subject, and the brain activity is buffered then fed into two operational amplifiers (AD8538, Analog Devices, Inc.) for appropriate amplification and band-pass filtering. A host computer stationed near-by is configured as a virtual instrument (VI) for remote real-time monitoring of spontaneous brain activities, while they are communicated based on a 2.4 GHz wireless IEEE 802.15.4/ZigBee protocol. The host computer, which is originally not capable of IEEE 802.15.4 communication, utilizes RS-232 to connect with a Texas Instrument SmartRF04 Evaluation Board with a CC2430 Evaluation Module for EEG data reception[23,24]. The core component on a microcontroller board is a CC2430 system-on-chip RF IC. The CC2430 integrates the CC2420 RF transceiver with an enhanced 8051 microcontroller unit (MCU), 128 KB flash memory, 8 KB RAM, and other peripherals [24].

3. Results and Discussion

3-1 Microstructural Analysis

Fig. 3(a) shows the hybrid hydrogels containing 54 wt % TEOS which were cross-linked by genipin with various weight ratios. After the CHC solution was incubated at 50°C in oven for 24 hours, the appearance of the hydrogels changed from transparent to light-green or dark-green. The UV spectra in Fig. 3(b) also demonstrate a corresponding variation in the color of the hybrid hydrogels. These results suggested that the CHC reacted chemically with genipin of a variety of concentrations displaying different color appearances and morphologies: the darker the color of the resulting hydrogels, the higher of cross-linked density of the hydrogels evolves.

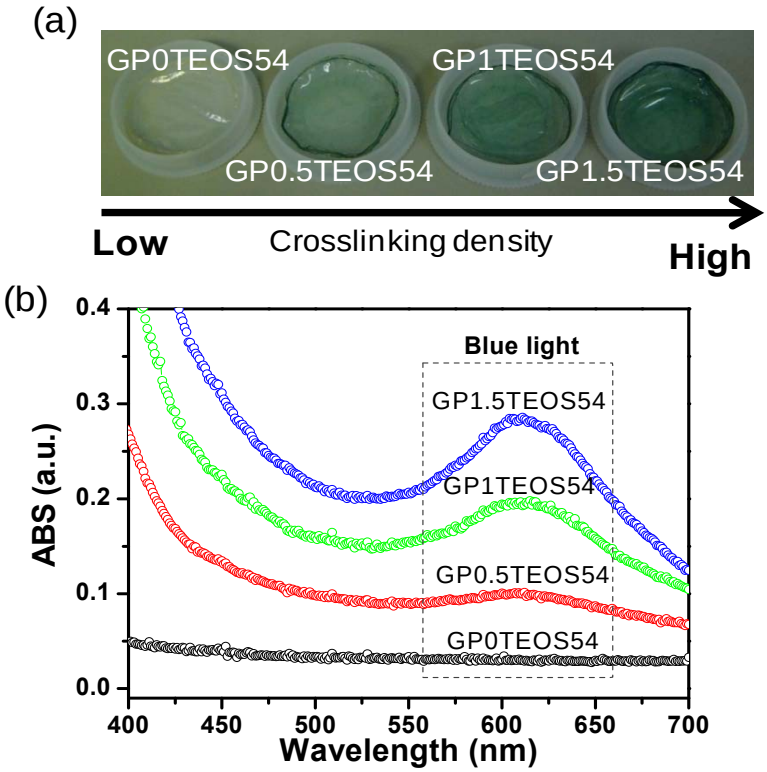

Fig. 3. (a) Optical photos of the hybrid hydrogels with different genipin cross-linked densities (b) UV spectroscopy analysis of different cross-linked hybrid hydrogels.

TEOS was hydrolyzed and condensed to form a network structure, which according to Liu et al. [25] may develop an interweaving network with CHC. The CHC hydrogels were crosslinked with various quantities of TEOS as shown in Fig. 4(a) where visual observation demonstrates that the resulting hybrid hydrogels, with constant concentration of genipin, showed similar appearance in color. Mechanical enhancement to the hybrid hydrogels can then be expected with higher TEOS content. In the meantime, the degree of cross-linking was increased, whilst the mesh size of the resulting hybrid network reduced, making the hybrids more compact. However, higher TEOS content deteriorated desired mechanical performance by imparting brittleness to the resulting hydrogels because of the formation of a continuous rigid silicate network. The thermogravimetric analysis (TGA), Fig. 4(b), of GP1.5TEOS0, GP1.5TEOS27, GP1.5TEOS54, and GP1.5TEOS70, shows that these four samples with different TEOS contents underwent a two-step thermal degradation process. The first degradation stage occurred at 30°C~120°C is due to evaporation of residual water and solvent which attributed to about 13.5% of weight loss. Above 200°C, the CHC polymer started to decompose, resulting in a decreased weight-loss curve. The crosslinking density can be calculated by the weight loss (%) at 500 °C, where the residues could be contributed solely by inorganic TEOS phase. On this basis, it is concluded that the crosslinked density for the TEOS-incorporated CHC, with constant genipin content at 500°C is decreased in the order of GP1.5TEOS70 > GP1.5TEOS54 > GP1.5TEOS27 > GP1.5TEOS0. This finding explicitly indicates that (1) the presence of silicate phase in the resulting hybrid hydrogels provides considerable thermal stability and (2) the higher TEOS, the higher cross-linking density results. For the latter, it is clear that a chemical interaction occurred between TEOS and CHC, which most plausibly through a dehydration between hydroxyl group of the hydrolyzed TEOS and carboxyl group along with the CHC chains.

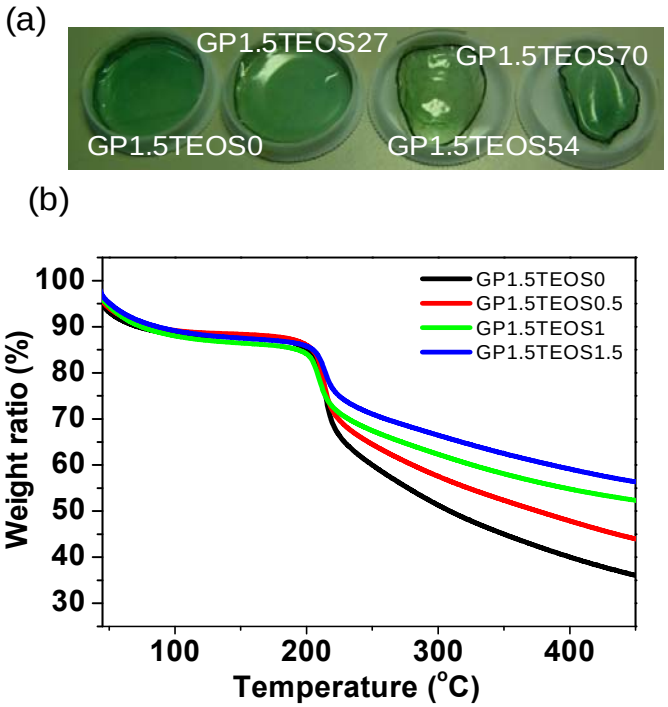

Fig. 4 (a) OM photos of the hybrid hydrogels with different TEOS cross-linked densities (b) TGA profiles.

In addition, morphological examination of the surface of the hybrid hydrogels displayed a change from relatively smooth texture for the hybrid hydrogel crosslinked by 0% - 0.5% GP, i.e., Fig. 5(a), whilst a winkled texture was detected with increased GP content, Fig. 5(b) and a more pronounced winkled surface was observed with 1.5% GP, i.e., Fig. 5(c)., With the same content of 1.5% GP, Figs. 5(d) and (e) show that the hybrid hydrogels with TEOS of 27% and 54%,

respectively, demonstrate winkled texture. However, considerable cracks and voids evolved along the hybrid surface when the highest-concentrated TEOS, i.e, 70%, was employed, GP1.5TEOS70, Fig. 5(f), which is due to an increase in brittleness of the resulting hybrid hydrogels, leading to cracking, rather than warping, upon drying.

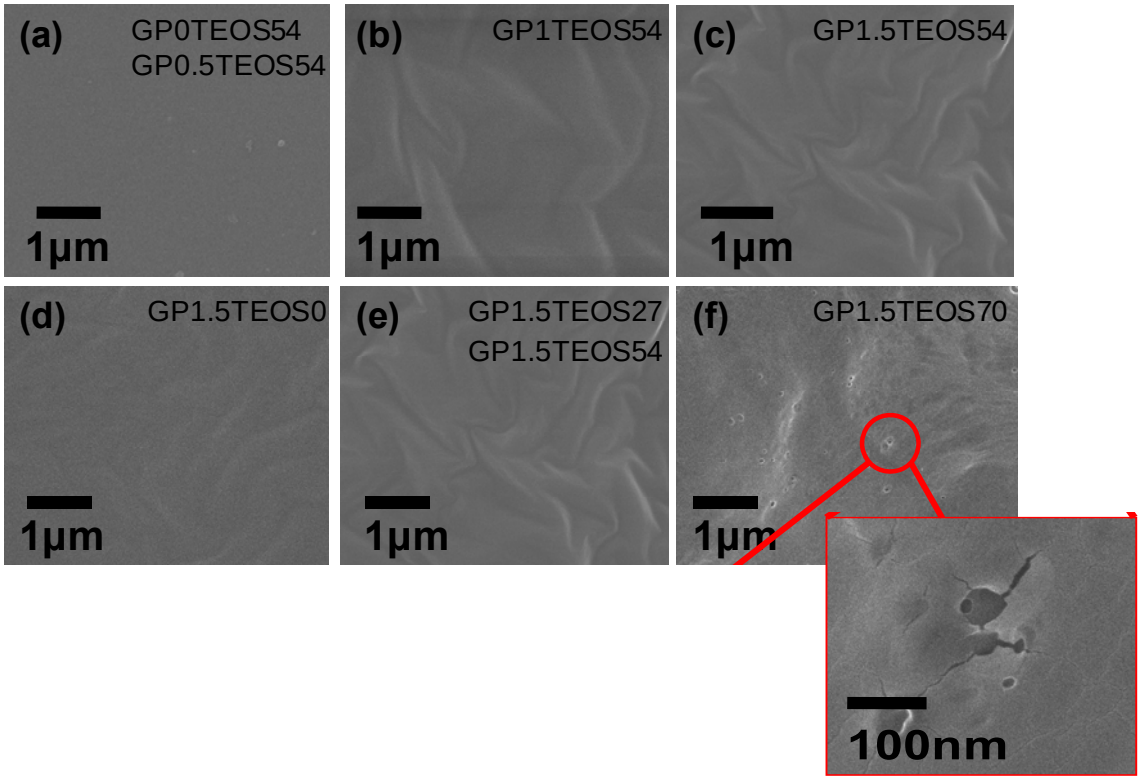

Fig. 5. The surface morphologies of CHC hydrogels crosslinked by different concentrations of genipin showed (a) a flat surface for the hydrogels containing 0%GP and 0.5GP , (b) a winkled surface and (c) a more winked surface with 1.5% genipin. The surface texture of the hybrid hydrogels with different contents of TEOS, 27%, 54%, and 70%, together with a fixed amount of 1.5% genipin, shown in (d), (e), and (f), respectively.

The swelling behaviors of the hybrid hydrogels with different degrees of cross-linking by genipin and TEOS are illustrated in Figs. 6(a) and (b), respectively. The profiles of GP0TEOS54 and GP1.5TEOS0 showed some specificity that both swollen hybrid hydrogels were hard to reach the swelling equilibrium but tended to collapse while immersing into water over a short period of time. It has known from previous study that CHC exhibits an excellent water affinity behavior at pH 7.4. In the absence of any crosslinking agents, the CHC was found to swell extensively till reaching a structural failure (collapse). Such structural failure is probably resulting from dis-assembly of the CHC polymer chains as a result of dissolution to form micelle entities in water. Similar structural dis-assembly was also observed from the hybrid hydrogels using either 54% TEOS alone or 1.5% genipin, as given in Figs. 6(a) and 6(b), respectively. It is then suggested that the hybrid hydrogels containing either TEOS or genipin alone were still subjecting to collapse upon extensive water absorption. However, what is more interesting is that the swelling behavior for the hybrid hydrogels with the use of both TEOS and genipin such as samples of GP0.5TEOS54, GP1TEOS54, GP1.5TEOS54, GP1.5TEOS27, GP1.5TEOS54, and GP1.5TEOS70, as given in Figs. 6(a) and (b), reaches equilibrium state for a longer time period of 45 minutes before a final structural collapse occurred. That is to say, the presence of both TEOS and genipin in the hybrids has more pronounced effect to strengthen the structure of the hybrids from undesirable mechanical failure upon swelling than their individual contribution. As

such, the swelling equilibrium can be achieved over a prolonged duration while structure integrity remained identical, rather than collapsed upon extensive swelling.

However, increase in the concentration of both genipin and TEOS decreased the swelling ratio of the resulting hybrid hydrogels. The swelling behavior in Fig.6 (a) indicates that samples of GP0.5TEOS54, GP1TEOS54, and GP1.5TEOS54 (i.e., hybrids with constant TEOS) have a swelling ratio, decreased with genipin content, of 427%, 354%, and 269% respectively. For samples with constant genipin, GP1.5TEOS27, GP1.5TEOS54, and GP1.5TEOS70 having a swelling ratio, decreased with TEOS content, of 550%, 326%, and 300%, respectively. It is then concluded that the higher content of the crosslinkers, the lower the swelling capability of the CHC hybrids results. The mesh size of the swollen CHC chains should accordingly be reduced proportionally.

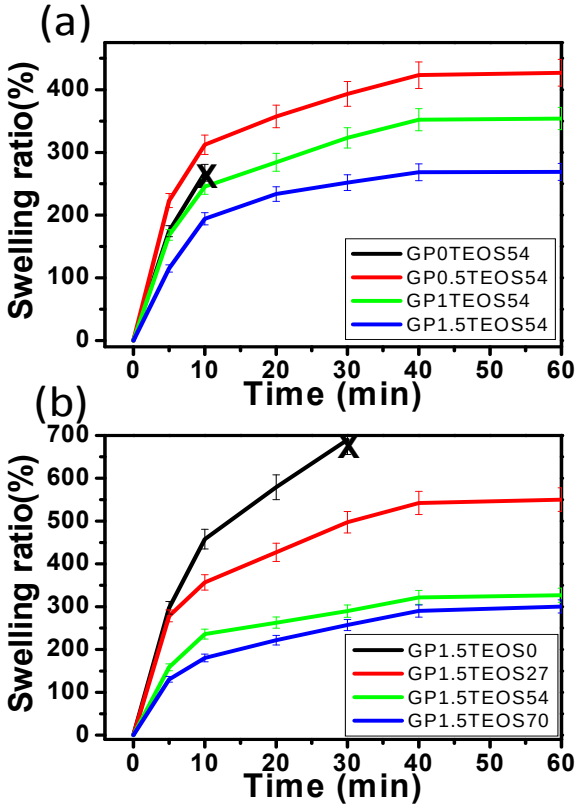

Fig. 6. Swelling behavior of the hybrid hydrogels with different contents of (a) genipin and (b) TEOS, as a function of time.

3-2 Drug Release Behavior from the Hybrids

ESM is water soluble and thermally stable drug, which is suitably employed for controlled release study and was employed as model molecule in this work. The in-vitro release of ESM from the CHC hybrids was measured over a 60-min period in deionized water, as shown in Figs. 7 (a) and (b). CHC hybrids with either TEOS or genipin alone illustrated a burst-like profile where the ESM was nearly completely eluted within 15 minutes. However, for hybrids such as GP0.5TEOS54, GP1TEOS54, GP1.5TEOS54, GP1.5TEOS27, GP1.5TEOS54, and GP1.5TEOS70 exhibited much slower release profile when both TEOS and genipin were incorporated with a higher concentration in either genipin or TEOS into the hybrids. The slower release profile for the hybrids with higher crosslink density can be resulting from a smaller mesh size of the hybrid networks than those hybrids with lower or little crosslink. The evolution of smaller mesh size in the network structure of high-crosslink hybrids may then be used to explain a lower diffusion rate for the ESM molecules to eluting outward. Hence, manipulation of the nanostructure of the hybrids has become a very important issue for designing a device suitable for controlled release of ESM.

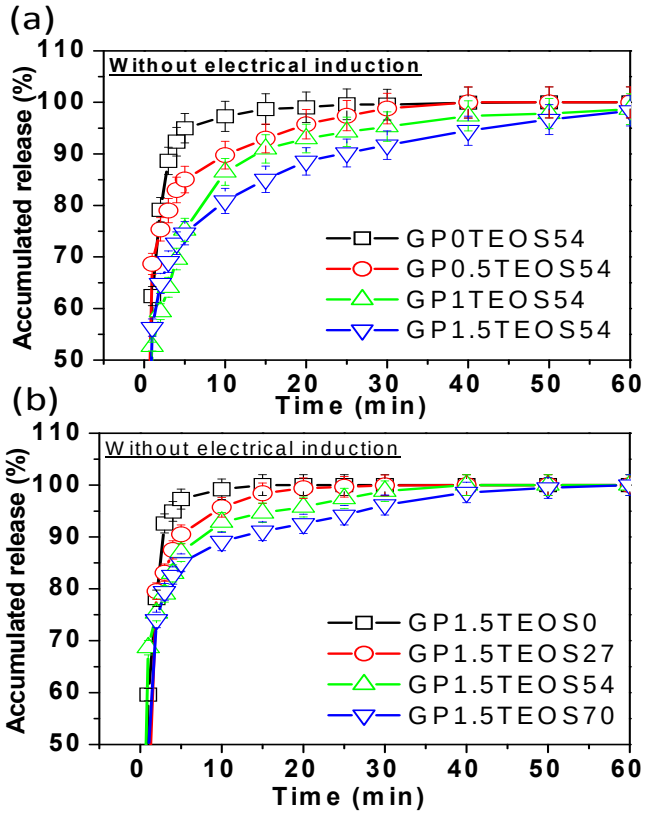

Fig. 7. In-vitro release of ESM from the hybrid hydrogels with **(a)** different genipin contents and **(b)** different TEOS contents.

3-3 Drug Release Behavior of the Device under Electric Field

I. Effect of genipin

Fig. 8(a) shows the in-vitro release of ESM from GP0TEOS54 hybrid which was integrated into a membrane-like configuration (hereinafter termed "chip"), under an applied electric field of different DC voltages from 0V to 60 V. It can be observed that the ESM was completely depleted over a time period of 120 minutes under zero voltage. Compared to Fig. 7(a), it indicates that when the hybrid hydrogels were inserted into the closed container, a full-scale swelling of the hybrids was effectively inhibited due to a constrained space. Since the swelling of the hybrids sandwiched in the container is heavily restricted, a subsequently restriction of the drug diffusion out of the chip is expected as a result of smaller mesh size developed within the hybrid hydrogel, resulting in a much slower release kinetics.

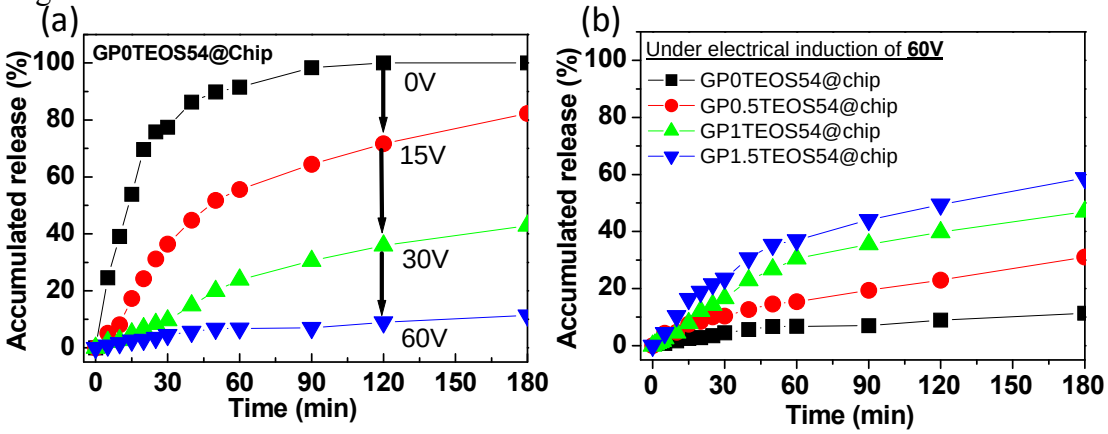

Fig. 8. (a) The ESM release profiles from GP0TEOS54 when applied DC electric field was operated as 0V, 15V, 30V, and 60V. (b) The release profiles with different genipin content under electrical operation of 60V.

Under electrical stimulus at voltages of 15V, 30V, and 60V respectively, drug release was restricted considerably with increased voltage, where only ~15% of ESM being eluted over a period of 180 minutes under 60-V electrical stimulus. Such an electrical-field-modulated ESM release profile can be presumably considered as a result of both electrophoretic and electroosmotic actions interplaying between the hybrid and ESM.

The chemical structure of ESM, with a molecular mass of 141.2 g/mole, has a chiral framework containing a five-member ring, with two negatively charged carbonyl oxygen atoms with a ring nitrogen between them and one asymmetric carbon atom, as shown in Fig. 9. Normally, it is more stable for ESM to perform with the structure of dehydrogenation. It means that the electron resonance between two carbonyl oxygen atoms and dehydrogenated nitrogen atom will give rise to a negatively charged ESM, which has been verified by ELS where its zeta potential is given in Table 2. Hence, upon application of an electrical stimulus, the H^+ ion, located at the nitrogen of ESM, preferred to escaping and being reduced at the cathode surface. In the meantime, the ESM molecules, which lost proton, should display electrophoretic movement to the anode because of strong negative charges. On the other hand, the immobile negative charges on the CHC polymer chain are exposed to an attractive force to positively charged H^+ ions formed as a result of the electrolysis of water or dehydrogenation of ESM in the presence of electric voltage. These H^+ ions forming a cloud of ions will enclose the polymers. Upon the application of electrical voltage, the positive H^+ ions surrounding the polymers will begin to move toward the anode with attractive force. Then the water molecules together with the ESM will be dragged toward the cathode by ion flow according to the gradient of ion and osmotic pressure, forming electroosmosis flow. Since the two forces, electrophoresis and electroosmosis, drive ESM movement toward the opposite direction, the net release of the drug from the hybrids is largely restricted (Fig. 9) [26-28]**.** Hence, electric current decreased the rate of drug release. With the increase of the applied voltage, those aforementioned effects turned out to be more pronounced, giving rise to a much slower rate of drug release. Therefore, it can be concluded that the electric field provided a net constrained force for ESM to diffuse out of the chip due to the interactive actions of both electrophoresis and electroosmosis.

Moreover, with an increase in genipin, the release profiles under electrical stimulation at 60V, in Fig. 8(b), show a faster release pattern. This observation is contrary to that in the absence of electrical stimulus. This behavior can be explained that at acidic condition, genipin reacted with primary amino groups on chitosan to form heterocyclic amines [28], the reaction will reduce the positive charges on the polymer chains. It is reasonably to believe that the same reaction scenario can be re-produced in the CHC chain. On this basis, higher crosslink density of the CHC chains with genipin leads to a stronger negatively charged CHC polymeric network. Thus, the effect of electroosmosis, which also facilitates gel shrinkage, should be enhanced, as has been verified in Ref.[26]. Under such an action, the ESM is forced to move outward the hybrids, and the chip as well, leading to a faster release profile as the genipin content increased.

Table 2. Zeta potential of Ethosuximide at different pH values.

pH values	Zeta potential of ESM (mV)
4	-9.82
7	-21.2
10	-45.7

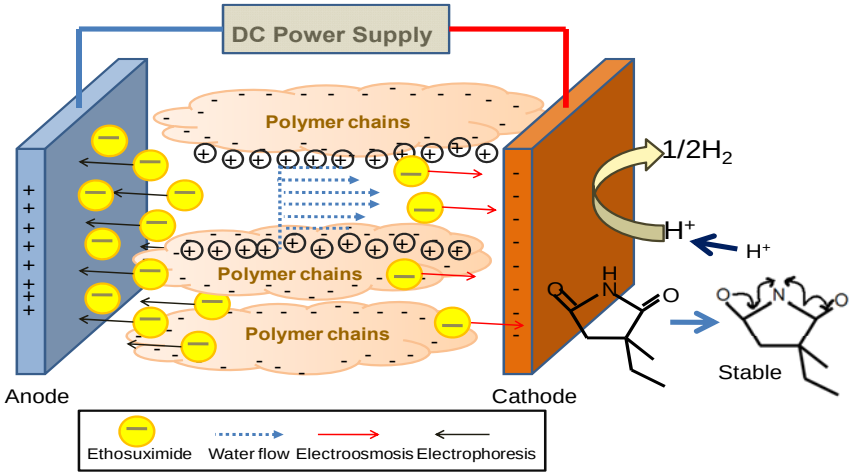

Fig. 9. The schematic drawing shows the influence of applied electrical voltage upon interactive actions between the ESM and CHC chain.

II. Effect of TEOS

Fig. 10(a) shows the elution of ESM from the GP1.5TEOS0-containing chip when the electric field with different voltages was applied. The release profile shows a complete depletion of the drug over a time period of 120 minutes**,** which is much slower than those illustrated in Fig. 7(b), where increase in the TEOS in the hybrids causes a decrease in the release profile. Such a change in ESM elution behavior as a function of TEOS content is also similarly observed in the case aforementioned, where, for the former, the swelling of the hybrids is largely restricted in the presence of TEOS and thus, reduced considerably the ESM diffusion from the hybrids.

Under electrical stimulus at 15V, 30V, and 60V, drug release rate was getting slower with the increase of voltage. This behavior can also be explained as an interplay between electrophoretic and electroosmosis actions aforementioned. The electrophoretic flow of ESM moves toward the anode but the electroosmotic flow carrying ESM toward the cathode, the opposite and competing actions restrict drug flow considerably out of the chip, resulting in a decreased ESM elution profile.

However, there seems to have an upper limit for the TEOS content in terms of the ESM elution behavior because from experimental observation, shown in Fig. 10(b), a continuous increase of TEOS to a certain critical level, i.e., 54 wt%, in the hybrid, the ESM elution turned faster, which is exactly contrary to what was detected for the hybrids without electrical stimulus. Such a finding can be explained that a more negative charge imparted to the CHC polymeric networks when more TEOS or silica was incorporated. The action of electroosmosis is then enhanced, which further contracts the resulting hybrid hydrogel to a certain extent under identical electric voltage, thus, resulting in a faster ESM elution rate.

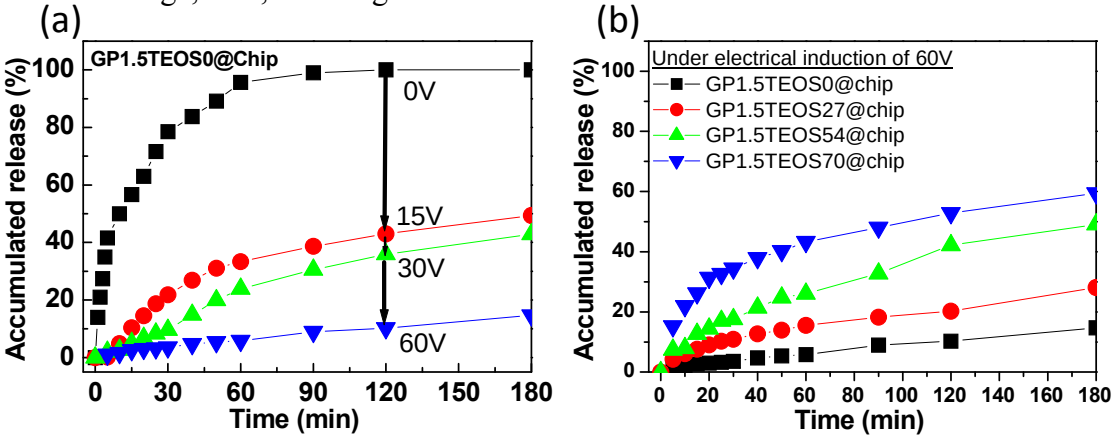

Fig. 10. (a) The ESM release profiles from GP0TEOS54 when applied DC electric field operated at 0V, 15V, 30V, and 60V. (b) The release profiles with different genipin content under electrical operation of 60V.

3.3 In-vivo study

To confirm the applicability of the chip to practical uses, the hybrid hydrogel with a composition of GP1.5TEOS54 was selected because of its sufficiently mechanical reliability and drug elution capability, according to in-vitro test, Fig. 10(b). In this preliminary in-vivo study, a unique design by integrating the biological self-detection and response-induced features of the chip on epileptic treatment was demonstrated. The architecture of the whole drug delivery system is shown in Fig. 11. The drug delivery system consists of four units: (a) signal acquisition and amplification unit, (b) 8051 micro-processor and wireless data transmission unit, (c) electric field and drug delivery chip, (d) host system for data storage and real-time display.

It can be observed in Fig. 11(a) that electroencephalogram (EEG) signal of the rat's frontal cortex is amplified and band-pass filtered (1000x, 0.3-80 Hz) by the op-amp, and then the amplified EEG is positive-biased to the input voltage range of an analog-to-digital converter (ADC) (Texas Instrument CC2430 chip). Thus, several tasks were implemented on the microcontroller board (MCU) (refer to Fig. 11(b)), including analog-to-digital conversion of EEG signals, execution of seizure detection, generation of trigger to the drug releasing chip, and EEG data wireless transmission. The MCU was programmed to control the sampling period of the ADC and the generation of trigger, retrieved the direct memory access (DMA) data, and started a series of feature extraction and seizure detection. The system detected epileptic seizures and immediately feedbacks to stimulate electric at the drug releasing chip (refer to Fig. 11(c)) to induce drug elution. Electric filed activated the structural change of the hybrid hydrogel in the chip to release drugs accordingly. Therefore, the controlled release system is regarded as a closed-loop drug delivery system on epilepsy control, as shown in Fig. 11(a)-(c). Furthermore, in order to achieve real-time monitoring, the real-time on-line seizure monitoring was developed using National Instrument LabVIEW to create a graphical user interface (GUI) VI to monitor and store the EEG data(refer to Fig. 11(d)).

A complete view of the backpack and of its placement on a rat is given in Fig. 12(a). There are two batteries in the backpack. In order to minimize the weight of head mounted devices for a rat, the backpack was mounted on the rat's jacket which was connected to the neural interface by short soft wires. Generally, the shorter the wires, the lower the noise picked from the environment. The detailed caption was given in Fig. 12(b), the neural interface consists of op-amplifier and constant voltage circuits. On the other hand, the microcontroller board used Texas Instrument CC2430 chip to compute detection epileptic seizure. When the MCU detects epileptic seizures, it would feedback immediately to trigger chip to release drug into the rat during eight minutes. The funnel chip can be demonstrated in the inset of Fig. 11(c).

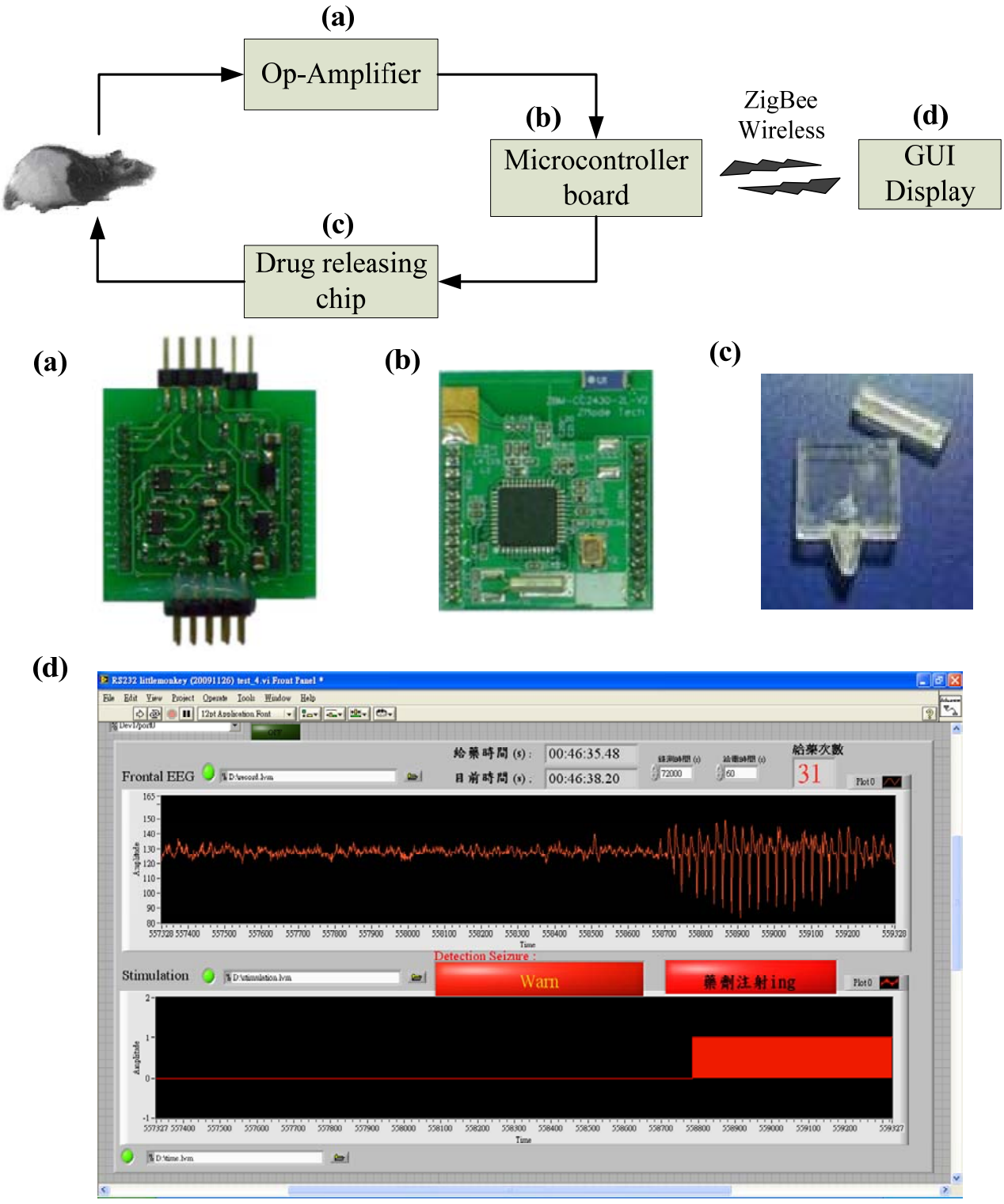

Fig. 11. Schematic illustration of the controlled release system. (a) signal acquisition and amplification unit, (b) 8051 micro-processor and wireless data transmission unit, (c) drug releasing chip, (d) host system for data storage and real-time display.

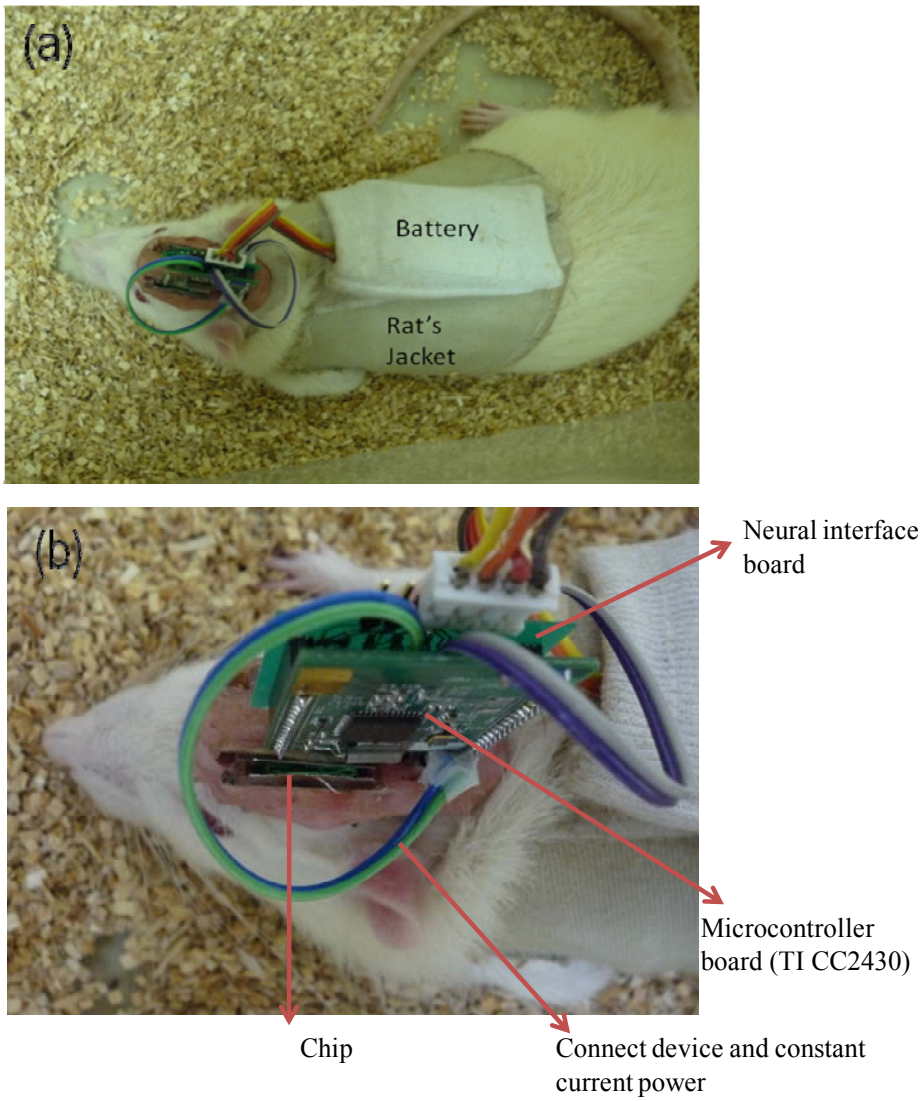

Fig. 12. Experimental setup of the animal study and the illustration of the drug release system, where the "chip" (b) indicates the drug delivery device.

Fig. 13 represents one example of the SWD of the rats in this experiment. We recorded 40-minutes spontaneous brain activity during released process and 20-minutes spontaneous brain activity after treatment. Fig. 13 demonstrates that the SWD of the rats reached ~120 times without drug administration while the SWD of the rats reduced by nearly 50% while ESM was released from the self-detection drug delivery system. Although it is hard to quantify the exact amount of the ESM release into the rats during the in-vivo operation, it is truly indicated that certain effective dose of ESM was released into the rats from the chip-based drug delivery system, which, for the first time, proved the concept of the integrated system designed based on the electrical-responsive hybrid hydrogel. Although this in vivo study has far from being optimized in terms of operation parameters among different parts of the integral system, drug dose, and time of dosing, the preliminary in-vivo outcomes do provide promising perspective toward further investigation. It is highly expected by combing photolithography technology frequently employed in semi-conductor industry, the implantation of the chip-based system would be expected to offer self-detection and effective therapeutic treatment for epileptic patients, and those who suffers from chronic diseases, in the future.

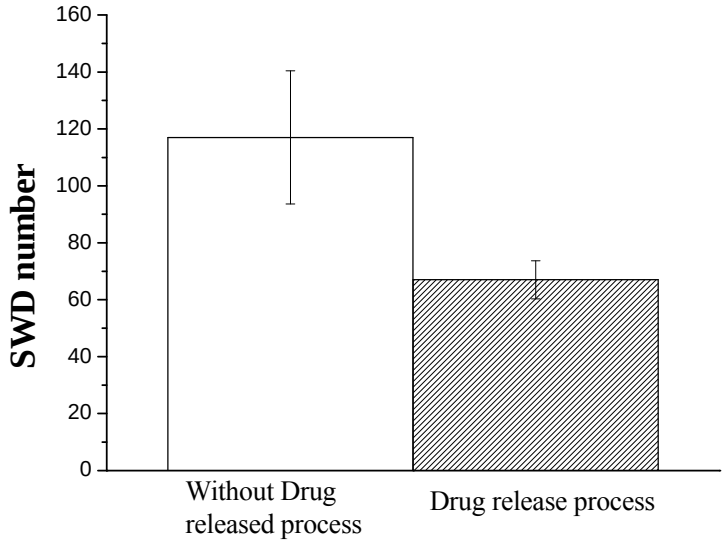

Fig. 13. Comparison of SWD number of the rats (n=6) with and without (as control group) drug elution from the chip-based drug delivery system.

4. CONCLUSION

This study demonstrates the synthesis of a hybrid hydrogel consisted of a modified chitosan and inorganic silica gel via a sol-gel route. The hybrid hydrogel showed improved thermal stability and mechanical swelling behavior, indicating an interaction evolved between the modified chitosan, i.e., carboxyl groups, and inorganic siliate phases, i.e., hydroxyl groups. An anticonvulsant drug, ESM, released from the hybrid, was evaluated in vitro under DC electric field of various voltages, showing different release profiles. The field-induced release mechanism from the hybrid hydrogels appeared to be a combined contribution between electrophoretic and electro-osmotic operations upon the electric field stimulus. While integrating the electric-responsive hybrid hydrogel, as a drug reservoir, into a self-detection system, we have successfully demonstrated a real-time responsive drug delivery operation in an epileptic rat model where the number of seizure was reduced considerably by ~50%, from automatic seizure detection to a subsequent release of anti-epileptic drug from the hybrid hydrogel, achieved in tens of seconds.

Acknowledgment

The authors gratefully acknowledge the financial support of the National Science Council in Taiwan through Contract NSC-98-2627-B-009-001.

References

[1] D. Shi, Adv. Fun. Mater. . 19 (21) (2009) 3356-3373.
[2] T. M. Allen and P. R. Cullis, Science. 303 (2004) 1818-1822.
[3] M. R. Prausnitz, S. Mitragotri, R. Langer, Nature Reviews Drug Discovery, 3 (2004) 115–124.
[4] Jindrˇich Kopecˇek, European Journal of Pharmaceutical Sciences. 20 (2003) 1–16.
[5] S. Sershen, J. West, Advanced Drug Delivery Reviews, 54 (9) (2002) 1225-1235.
[6] F. Balas, M. Manzano, P. Horcajada, M. Vallet-Regi, J. Am. Chem. Soc. 128 (25) (2006) 8116–8117.
[7] D. A. Groves and V. J. Brown, Neuroscience Biobehavior, 29 (3) (2005) 493-500.
[8] N. Kannathal, M. L. Choo, U. R. Acharya and P. K. Sadasivan, Computer Methods and Programs in Biomedicine, 80 (3) (2005).
[9] V. Srinivasan, C. Eswaran, N. Sriraam, Information Technology in Biomedicine, 11 (3) (2007) 288-295.
[10] O. A. Rosso, Entropy changes in brain function, International Journal of Psychophysiology, 64 (1) (2007) 75-80.
[11] R. J. Racine, Electroencephalography and Clinical Neurophysiology, 3 (3) (1972) 81-94.
[12] F. Z. Shaw, Y. F. Liao, Journal of Neurophysiology, 93 (2005) 2435-2448.
[13] S. F. Liang, H. C. Wang, and Y. C. Liao, Proceeding of 13th International Conference on Human-Computer Interaction, San Diego, USA, (2009) 711-715.
[14] S. F. Liang, H. C. Wang, and W. L. Chang, EURASIP Journal on Advances in Signal Processing, (2010).
[15] Y. Qiu, K. Park, Advanced Drug Delivery Reviews, 53 (2001) 321-339.
[16] J. L. Drury and D. J. Mooney, Biomaterials, 24 (24) (2003) 4337-4351.
[17] T. Y. Liu, S. Y. Chen, Y. L. Lin, and D. M. Liu, American Chemical Society, 22 (23) (2006) 9740–9745.
[18] W. C. Huang, S. H. Hu, K. H. Liu, S. Y. Chen, D. M. Liu, J. Control. Release, 3 (139) (2009) 221-228.
[19] J. E. Lopez, N..A. Peppas, Journal of Biomaterials Science, Polymer Edition 15 (4) (2004) 385-396.
[20] F. Z. Shaw, Journal of Neurophysiology, 91 (2004) 63-77.
[21] C. P. Young, S. F. Liang, D. W. Chang, Y. C. Liao, F. Z. Shaw, and C. H. Hsieh, IEEE Trans. on Instrumentation & Measurement, (2010) (accepted).
[22] F. Z. Shaw, Journal of Neurophysiology, 97 (2007) 238-247.
[23] CC2430 software examples user's guide, Texas Instrument. [Online] Available: http://www.ti.com/litv/pdf/swru178.
[24] A true system-on-chip solution for 2.4 GHz IEEE 802.15.4/ZigBee (Rev. F), Texas Instrument. [Online] Available: http://www.ti.com/lit/gpn/cc2430.
[25] K. H. Liu, T. Y. Liu, S. Y. Chen, D. M. Liu, Acta Biomaterialia 4, 1038–1045 (2008).
[26] S. Ramanathan, L. H. Block, Journal of controlled Release, 70 (2001) 109-123.
[27] T. Tanaka, Gels, Sci. Am244 (1981) 124-138.
[28] J. P. Gong, T. Nitta, Y. Osada, J. Phys. Chem., 98 (38) (1994) 9583–9587.

Part-IV. 計畫執行績效:

就研究成果而言，目前本子計畫在2009~2010 已發表三篇論文著作於High-impact 國際期刊如下與一項專利申請:

Published Papers:

1. Yen-Po Chang, Kun-Ho Liu, Chih-Shin Chao, **San-Yuan Chen***, Dean-Mo Liu, Synthesis and characterization of mesoporous Gd2O3 nanotube and its use as a drug-carrying vehicle, **Acta Biomaterialia** 6 (2010) 3713–3719. (**IF=3.98**, N/M=5.1%)
2. Shang-Hsiu Hu, Kuan-Ting Kuo, Wei-Lin Tung, Dean-Mo Liu,and **San-Yuan Chen*** , A Multifunctional Nanodevice Capable of Imaging, Magnetically Controlling, and In Situ Monitoring Drug Release, **Advanced Functional Materials**, 19, 3396–3403 **(2009)** (IF=6.99, N/M=4.21%)
3. Wei-Chen Huang, Kun-Ho Liu, Shang-Hsiu Hu, **San-Yuan Chen*** and Dean-Mo Liu, "A Flexible Drug Delivery Chip for Magnetically-Controlled Release of Anti-Epileptic Drug", **Journal of Controlled Release 139 (3), 221-228, NOV (2009)** (IF=5.949, N/M=5.90%)

Patent Application:

應用於慢性疾病的生物自我偵測及回饋誘導藥物釋放系統
申 請 日：民國99 年9 月15 日
申請國家：中華民國、美國
案件類型：發明

2010 年第八屆國際新藥發明科技年會 與 第一屆奈米醫藥大會

8th Annual Congress of International Drug Discovery Sciences and Technology

1st Annual World Congress of Nanomedicine-2010

陳三元　教授

國立交通大材料科學與工程學系所

(一)參加會議過程：

本人於 2010 年 10 月 22 日早上(AM 8:00) 從桃園國際中正機場搭乘華航航空客機前往中國大陸北京(Beijing)，到北京時已經是下午，覺得蠻好的，接著就住進旅館，並立即前往會場並辦理報到註冊手續。然後就是一系列密集又緊湊的三天研討會，於 10 月 25 日中午結束研討會，然後再從北京機場搭機，經香港國際機場轉機，再搭乘華航航空客機，飛回臺灣桃園國際中正機場，此時已經是下午 7:30，到家之後又要忙著到學校上課，因此覺得相當的累，但是精神還算不錯。在此仍是非常感謝國科會的補助，能參加這次奈米科學與技術及奈米醫藥的國際性研討會議，心裡覺得很高興，畢竟此種經驗是很難得的，希望藉此次的參與，能多吸取別人的優點及經驗，以便對日後的研究會有所幫助。

這次第八屆國際新藥發明科技年會 與 第一屆奈米醫藥大會，是由中國大陸的國家奈米科學與技術中心所主辦並且有其他重要研究中心及期刊贊助。這個會議主要是強調奈米科學材料及技術之跨領域的學術研究及應用—以發展具有利基(cutting-edge) 奈米技術、材料與元件。國際新藥發明科技年會的內容主要涵蓋Basic Sciences and Technologies of Drug Discovery, Emerging Technologies and Key Tech Platform Infrastructure for Drug Discovery, Advances in Anti-Major Disease Drug R

& D, Smart Medicinal Chemistry toward NCEs , Innovations and Improvement of Major Biotherapeutics, Tech-Upgrade of Key Drugs & Biosimilar Products, Scientifically Upgrading Key Chinese Traditional Medicines, Translational Medicine and Globalization Strategies, Professional Industrial Incubators for Drug Innovations等理論與應用技術，因此可以說是一個很受重視的國際學術會議之一。奈米醫藥大會則強調 Nanosciences and Leading Edge Nanotech in Nanomedicine, Nanobiotechnology, Nanopharmaceuticals, Advances in Nanomedicine, IT, Instrumentation and Equipment in Nanomedicine, Milestones of Applied Nano-medical Technologies, Breaking Research of Novel Engineering Systems in Nanomedicine, Regulatory, Ethic Issues and Business Outlook in Nanomedicin。

在今年的研討會中，共有來自 37 個國家，並有超過 1000 篇 Full papers 論文及 Poster 約 450 篇，出席的專家學者有近 1500 人，其中最特別的是準備兩場 Plenary Section，Dr. Erwin Neher, Title : signals and signaling molecules in the central nervous system. Dr. Christian Amatore, Title: Investing of oxidative stress at single cells with ultramicoelectrodes: A new platform for drug testing. 總共邀請 5 位國際在奈米等相關領域之著名的大師，針對一些重要奈米材料科學及技術的研究主題做一些深入探討及報導，覺得相當有收獲。同時另外則有 Posters，除此之外大會也安排一些重要廠商參展。由於這次是由兩個國際會議一起主辦故參與的學者相當多。來自台灣參與這次研討會，包括台灣大學、交通大學、長庚大學、師範大學、中山大學、及清華大學的學生與教授。

(二)與會心得：

此次研討會包括第八屆國際新藥發明科技年會 與 第一屆奈米醫藥大會等兩大國際會議一起主辦，因所發表論文的範圍，相當廣泛且內容非常豐富。本人亦發相當多的時間，在聆聽這些方面相關的研究論文發表，吸收一些別人的研究心得與資訊，以期爲未來的研究方向，做進一步的規劃及考量。在與會中，不僅碰到有一些有興趣的學者，也提出他們的觀點及問題與筆者深入探討，同時筆者也趁這個機會多看看一些相關其他的研究 Posters ，以進一步瞭解目前這方面的研究趨勢，從這些相互討論中確實能得到一些心得。

從這些所發表的論文及所聽聞的研究內容，可以看出目前或甚至未來在奈米及生醫材料的發展趨勢及重點，將會集中於 Molecule image, Nanopharmaceuticals, Bio-detector with nanotechnology, Nanomedicine and controlled release 與 Drug delivery and Tumor treatment，這與本人目前研究的重點相近，但是若進一步考量台灣的目前特殊環境，在臨床醫學的研究仍相當缺乏，但在光電相關科技，則相當發達，因此若從短中長期的研究規劃，可以看出則分別可定爲早期的生醫感測(biosensors/biodetectors)，中期的奈米生醫及藥物釋放控制與傳遞，到腫瘤早期偵測及治療、甚至到後期的組織工程與再生，這對我未來的研究將更顯得重要，這也是我參加這個會議的一個目的，希望能從這次會議，多聆聽一些有關這方面的研究。另外由於參與此次盛會的專家學者很多，所以在此種場合之下，除了專程參加會議發表論文之外，還需要適當地做一些社交的活動，認識一些同樣領域的學者，有時也盡量試著與一些大師級的學者交談，彼此交換研究心得，並且還可以吸收最新的研究資訊，對本身的研究工作會有所幫助。

(三)建議：

筆者非常感謝國科會的補助，才能參加此次的國際性學術研討會，藉由此次會議，可以促進國際間的學術交流，互相交換研究成果，以提高我們中華民國的學術地位及知名度。類似這樣很重要的國際性會議，應該多鼓勵及補助國內學者專家積極的參與。

(四)攜回資料名稱及內容：

此次參加會議攜回研討會論文摘要集，其內容涵蓋本次會議所發表的一些論文的重要研究結果及摘要。

無衍生研發成果推廣資料

98 年度專題研究計畫研究成果彙整表

計畫主持人：陳三元	計畫編號：98-2627-B-009-001-
計畫名稱：智慧型生物訊號誘導藥物釋放系統前瞻研究:以癲癇症為模式--應用於訊號誘導藥物釋放系統之智慧型生醫複合材料結構製程與性質研究(總計畫及子計畫二)(3/3)	

成果項目			量化			單位	備註（質化說明：如數個計畫共同成果、成果列為該期刊之封面故事...等）
			實際已達成數（被接受或已發表）	預期總達成數(含實際已達成數)	本計畫實際貢獻百分比		
國內	論文著作	期刊論文	0	0	100%	篇	
		研究報告/技術報告	1	0	100%		
		研討會論文	1	0	100%		
		專書	0	0	100%		
	專利	申請中件數	1	0	100%	件	
		已獲得件數	0	0	100%		
	技術移轉	件數	0	0	100%	件	
		權利金	0	0	100%	千元	
	參與計畫人力（本國籍）	碩士生	2	0	100%	人次	
		博士生	1	0	100%		
		博士後研究員	0	0	100%		
		專任助理	0	0	100%		
國外	論文著作	期刊論文	3	0	100%	篇	
		研究報告/技術報告	0	0	100%		
		研討會論文	1	0	100%		
		專書	0	0	100%	章/本	
	專利	申請中件數	1	0	100%	件	
		已獲得件數	0	0	100%		
	技術移轉	件數	0	0	100%	件	
		權利金	0	0	100%	千元	
	參與計畫人力（外國籍）	碩士生	2	0	100%	人次	
		博士生	1	0	100%		
		博士後研究員	0	0	100%		
		專任助理	0	0	100%		

其他成果 (無法以量化表達之成果如辦理學術活動、獲得獎項、重要國際合作、研究成果國際影響力及其他協助產業技術發展之具體效益事項等，請以文字敘述填列。)	1. 本子計畫符合執行進度。 2. 對於團隊間研究資料分享與配合為優。本計畫不僅提供子計畫二奈米藥物之動物測試平台，亦提供子計畫一自發性失神癲癇大鼠腦波以及 Amygdala 誘發之顳葉抽搐型癲癇之腦電波訊號。目前本計畫已進行電場式的奈米型 ESM 灌流裝置並完成初步實驗測試，已經發現在側邊大腦區域灌流奈米型 ESM 可以顯著地抑制失神性癲癇放電次數，其抑制效果並與劑量成正相關，此結果支持本計畫之初步假說。相信未來的密閉式回授藥物型癲癇抑制器將可以進行實際的大量動物測試，以做為人體臨床測試前之重要資料庫。

	成果項目	量化	名稱或內容性質簡述
科教處計畫加填項目	測驗工具(含質性與量性)	0	
	課程/模組	0	
	電腦及網路系統或工具	0	
	教材	0	
	舉辦之活動/競賽	0	
	研討會/工作坊	0	
	電子報、網站	0	
	計畫成果推廣之參與（閱聽）人數	0	

國科會補助專題研究計畫成果報告自評表

請就研究內容與原計畫相符程度、達成預期目標情況、研究成果之學術或應用價值（簡要敘述成果所代表之意義、價值、影響或進一步發展之可能性）、是否適合在學術期刊發表或申請專利、主要發現或其他有關價值等，作一綜合評估。

1. 請就研究內容與原計畫相符程度、達成預期目標情況作一綜合評估

■達成目標

□未達成目標（請說明，以 100 字為限）

□實驗失敗

□因故實驗中斷

□其他原因

說明：

2. 研究成果在學術期刊發表或申請專利等情形：

論文：■已發表 □未發表之文稿 □撰寫中 □無

專利：□已獲得 ■申請中 □無

技轉：□已技轉 □洽談中 ■無

其他：(以 100 字為限)

發表三篇於 Acta Biomater, Advanced Functional Materials, J. Controlled Release
目前尚有一篇正在 Joural of Controlled Release 審查中
至於誘導藥物釋放系統之材料結構的專利，已撰寫完畢並送學校智權處進行審核

3. 請依學術成就、技術創新、社會影響等方面，評估研究成果之學術或應用價值（簡要敘述成果所代表之意義、價值、影響或進一步發展之可能性）（以 500 字為限）

本技術主要是要發展一種具有智慧型快速反應型的藥物結構釋放系統，此智慧型載體因本身奈米複合結構具有高度的電磁敏感性，可感應來自當人體內部由於疾病發作時所產生的病理訊號或病徵，例如癲癇症的瞬間放電，經由無線訊號的判讀、偵測及轉換成為電場或磁場誘導之訊號，來刺激或啟動此智慧型奈米複合材料結構及形態的改變，進而釋放出適當藥物劑量，以達到有效疾病預防或治療的效果。這在學術上是相當創新並且此所研發之癲癇釋藥系統，也具有相當應用價值及貢獻。因為本研發主要技術特色在於能夠及時給予藥物來針對腦部發作的區塊做立即的抑制，不需要長時間施打藥劑，第二個特色是偵測的演算法寫入嵌入式開發板，直接在 TI CC2430 上運算，第三個特色就是有無線傳輸的功能可以立即觀測藥劑給藥情形與腦波訊號的變化。因此在未來若能進一步研發改良，相信這對於慢性疾病如癲癇症或糖尿病等的病人，在生活品質上將會大大提升。